Understanding the low-frequency electrical properties of ice–water interfaces from laboratory and field experiments

Clemens Moser[1], Alexander Bast[2,3], Sophie Francis[1], Matthias Halisch[4], Christian Hauck[5], and Adrián Flores Orozco[1]

3D orthomosaic

[Orthomosaic from Moser et al., 2025]

3D conductivity model

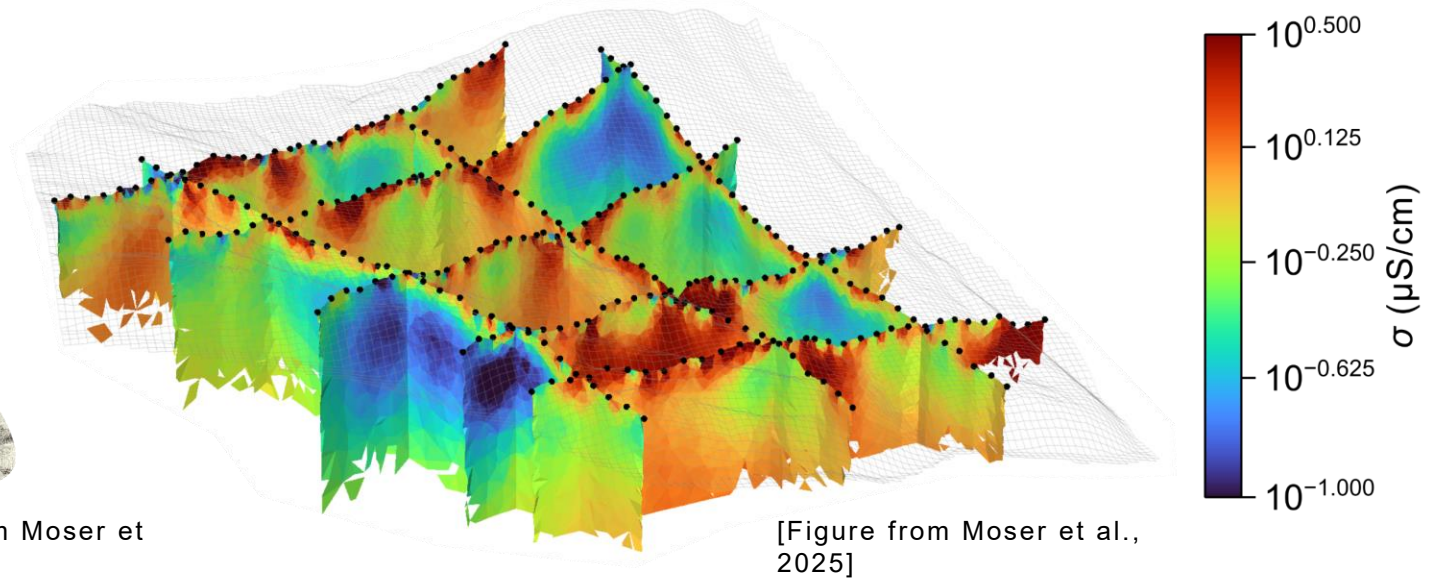

[Figure from Moser et al., 2025]

Electrical conductivity can be **ambiguous** in alpine permafrost
→ Use of **low-frequency polarization** effects as **complementary parameter**

[1]Research Unit of Geophysics, Department of Geodesy and Geoinformation, TU Wien, Vienna
[2]Permafrost, Alpine Environment and Natural Hazards, WSL Institute for Snow and Avalanche Research SLF, Davos Dorf, Switzerland
[3]Climate Change, Extremes and Natural Hazards in Alpine Regions Research Centre CERC, Davos Dorf, Switzerland
[4]LIAG Institute for Applied Geophysics, Dept. FA2.2 – Petrophysical Characterisation, Hannover, Germany
[5]Department of Geosciences, University of Fribourg, Fribourg, Switzerland

Spectral induced polarization experiments at three different scales

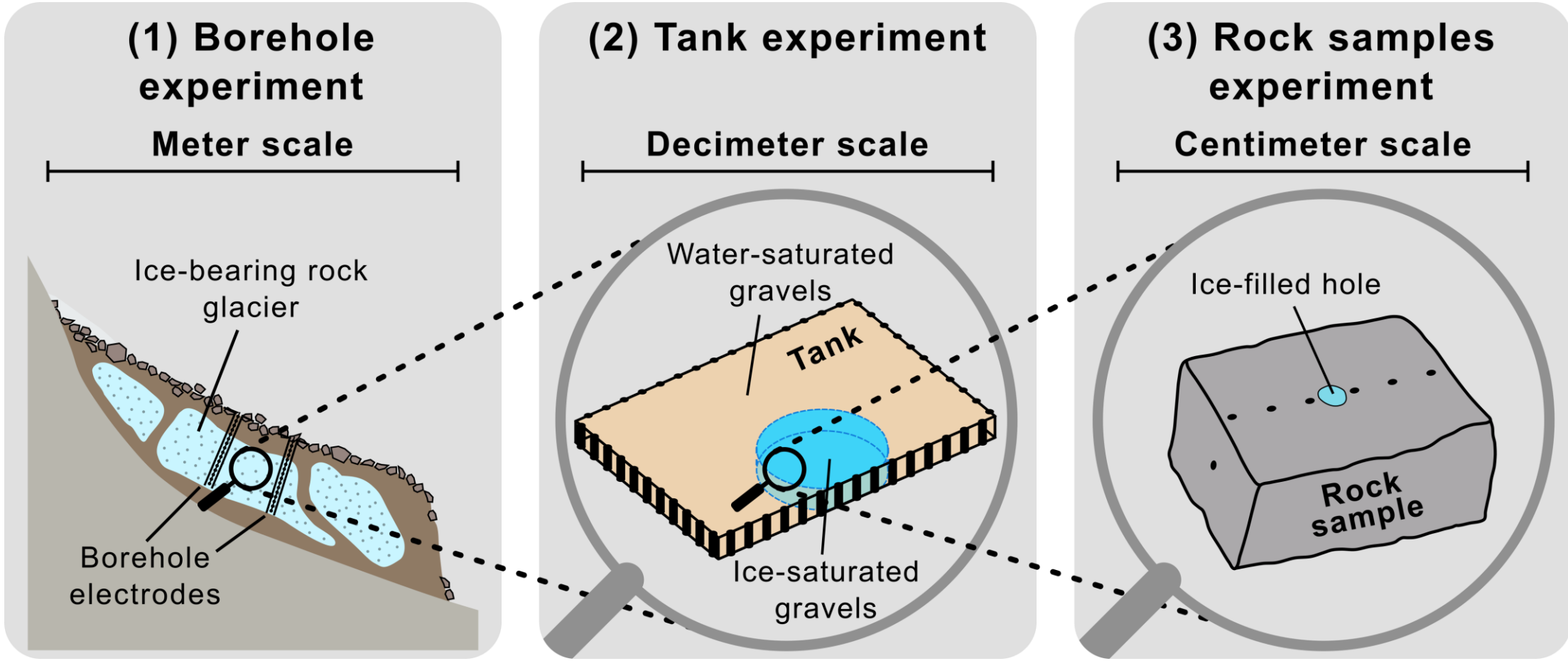

Understanding the low-frequency electrical properties of ice–water interfaces from laboratory and field experiments

Clemens Moser[1], Alexander Bast[2,3], Sophie Francis[1], Matthias Halisch[4], Christian Hauck[5], and Adrián Flores Orozco[1]

Context

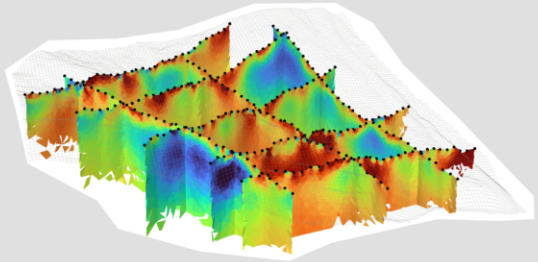

Spectral Induced Polarization Method

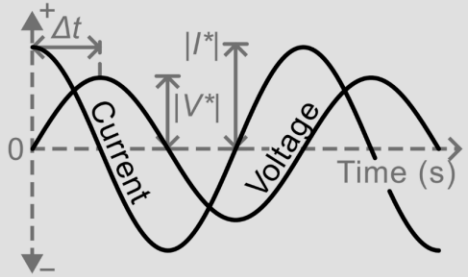

Experiments at different scales

(1) Borehole experiment

Meter scale

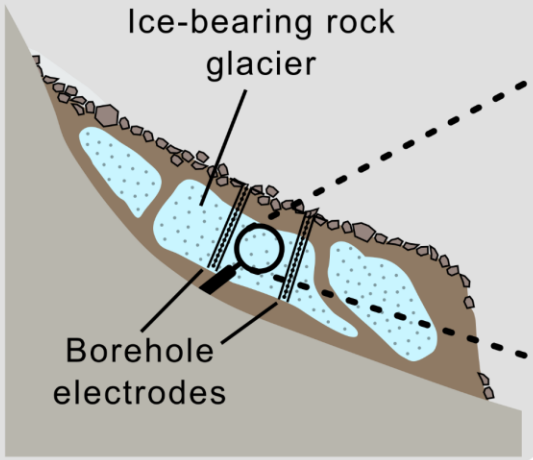

(2) Tank experiment

Decimeter scale

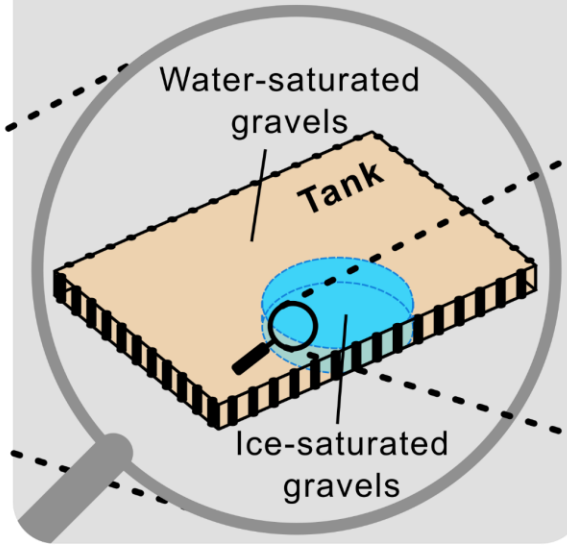

(3) Rock samples experiment

Centimeter scale

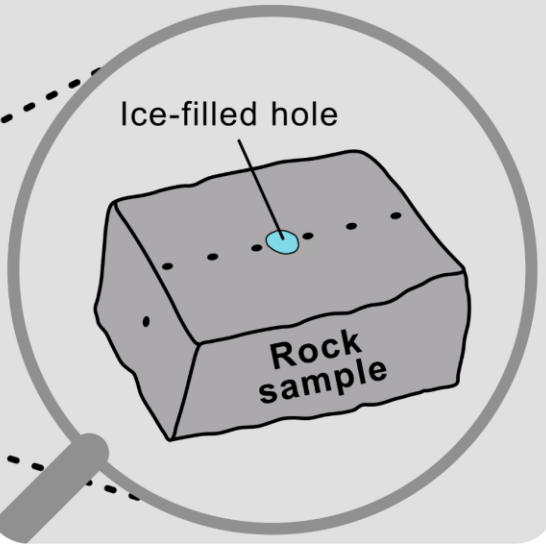

[1]Research Unit of Geophysics, Department of Geodesy and Geoinformation, TU Wien, Vienna
[2]Permafrost, Alpine Environment and Natural Hazards, WSL Institute for Snow and Avalanche Research SLF, Davos Dorf, Switzerland
[3]Climate Change, Extremes and Natural Hazards in Alpine Regions Research Centre CERC, Davos Dorf, Switzerland
[4]LIAG Institute for Applied Geophysics, Dept. FA2.2 – Petrophysical Characterisation, Hannover, Germany
[5]Department of Geosciences, University of Fribourg, Fribourg, Switzerland

Electrical methods for permafrost investigations

3D orthomosaic

[Orthomosaic from Moser et al., 2025]

3D conductivity model

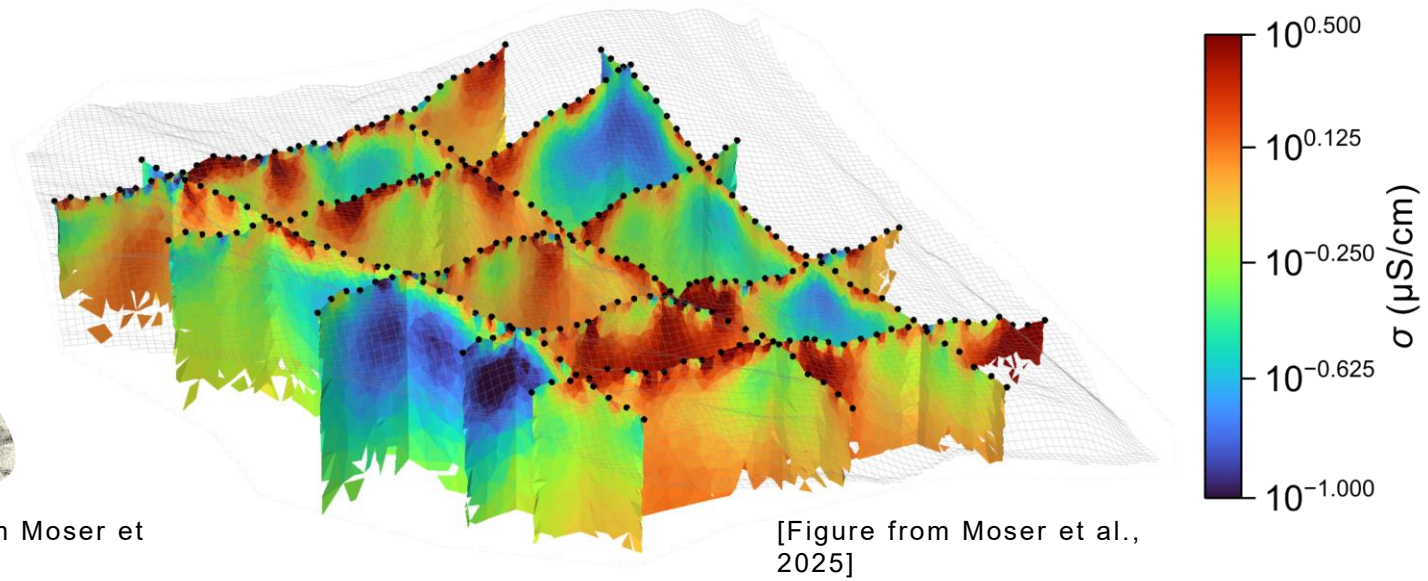

[Figure from Moser et al., 2025]

- **Geophysical methods** can provide information about **hydrogeological properties** (e.g., ice and water content) in the subsurface.
- Particularly, **electrical conductivity** is a well established parameter to **distinguish between frozen and unfrozen areas**.
- However, using **conductivity** alone may be **ambiguous** (rocks and ice can be both highly resistive).

Polarization effects in frozen materials

Pure ice

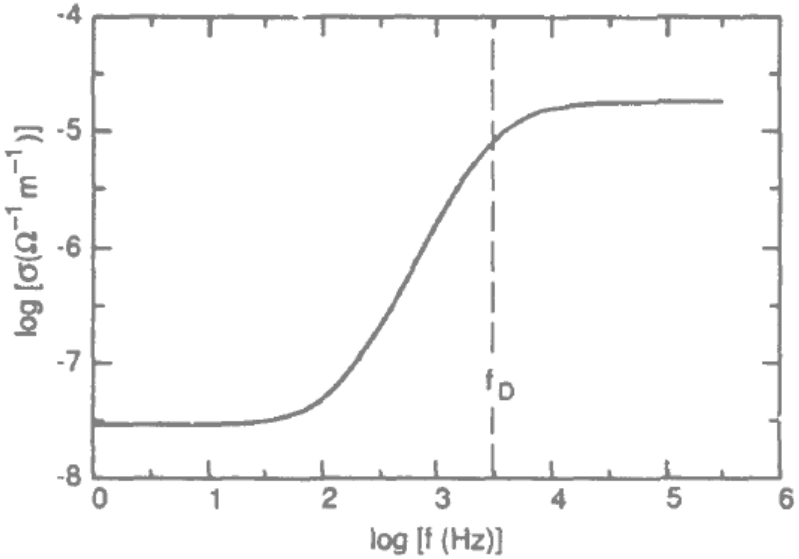

[Figure from Petrenko, 1993]

Exploitation of high-frequency effect at the field scale:

- Grimm & Stillman, 2015
- Mudler et al., 2024
- Sugand et al., 2026

Ice in solid rocks / sediments

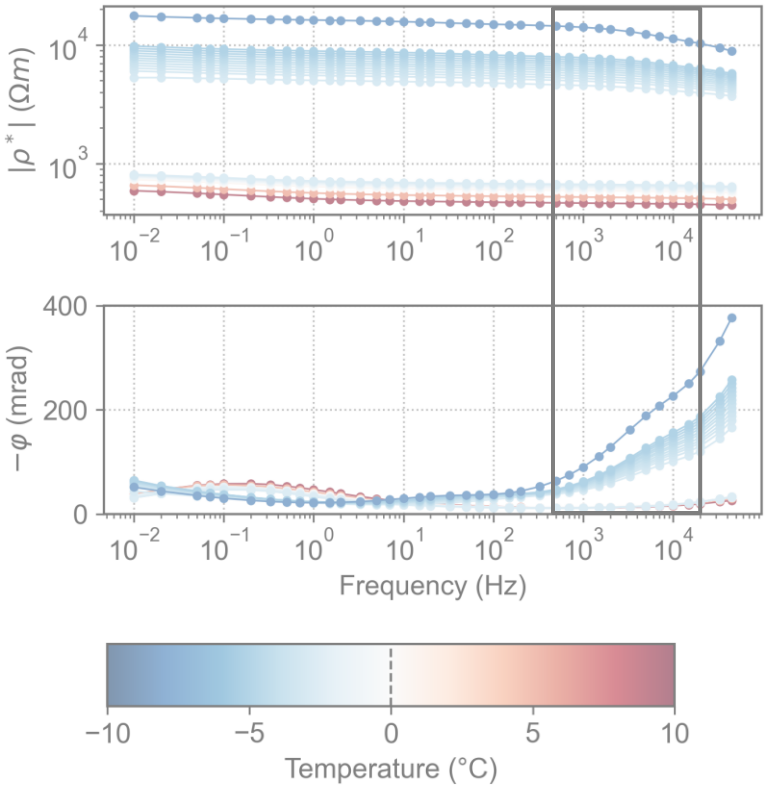

[Data from Limbrock et al., 2025]

Low-frequency effects

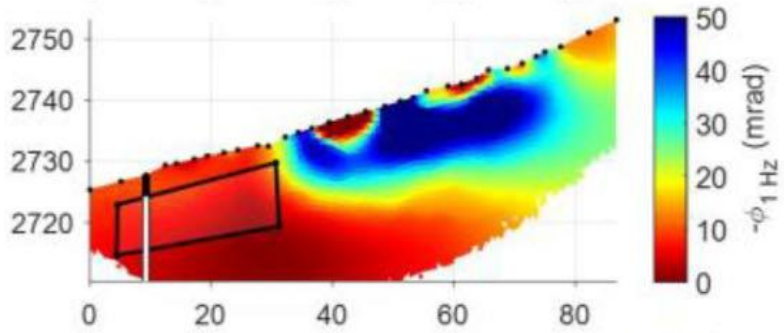

[Figure from Maierhofer et al., 2026]

This study

Hypothesis: The electrical double layer (EDL) formed at the ice–water interface results in a low-frequency polarization response (f < 1 kHz).

Three experiments at different scales to test this hypothesis.

Spectral Induced Polarization (SIP) method

Impedance measurement

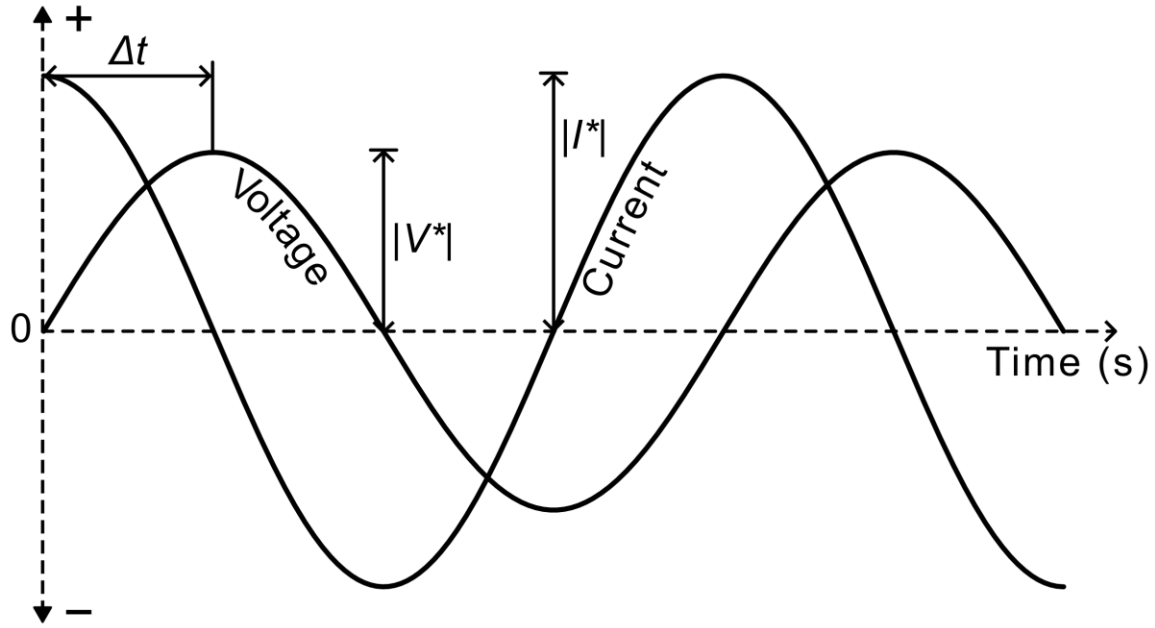

Impedance: $Z^* = \frac{V^*}{I^*} = |Z^*|e^{i\varphi}$

- **Magnitude:** $|Z^*| = \frac{|V^*|}{|I^*|}$
- **Phase:** $\varphi = 2\pi \frac{\Delta t}{T_p}$

Z^*... Impedance (Ω)
V^* ... Voltage (V)
I^* ... Current (A)
φ ... Phase (rad)
i ... Imaginary number

Complex conductivity

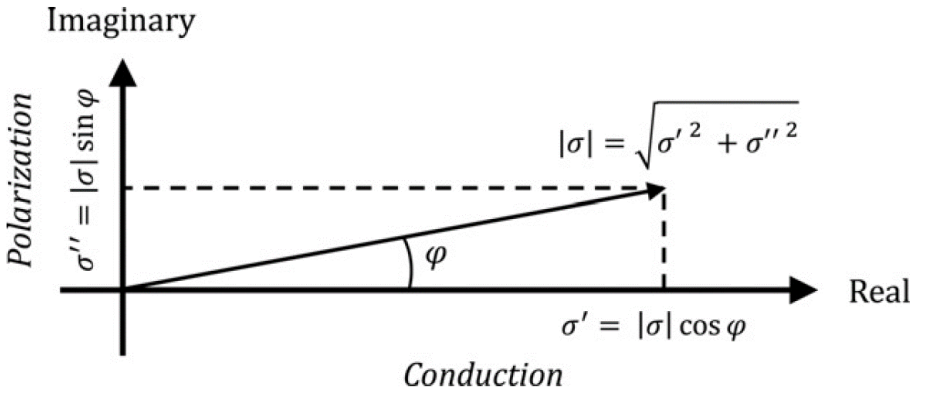

[Figure from Binley & Slater 2020]

$$\sigma^* = \sigma' - i\sigma'' = |\sigma^*|e^{i\varphi}$$

σ' ... Real part (S/m)
σ'' ... Imaginary part (S/m)
$|\sigma^*|$ ... Magnitude (S/m) ~ σ‘
φ ... Phase angle (mrad) ~ σ''/σ'

(3) Rock samples experiment

Centimeter scale

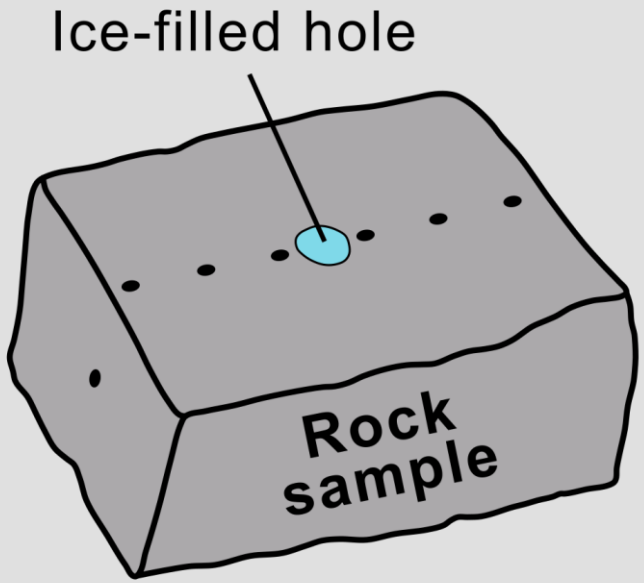

Experiment setup

(1) Drilling a hole

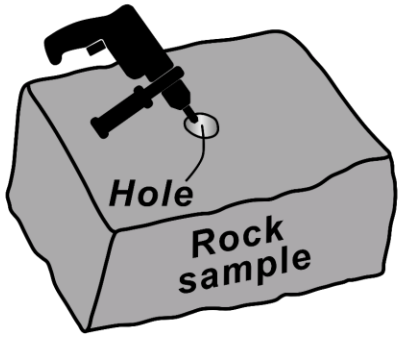

(2) Saturate the sample in a vacuum chamber

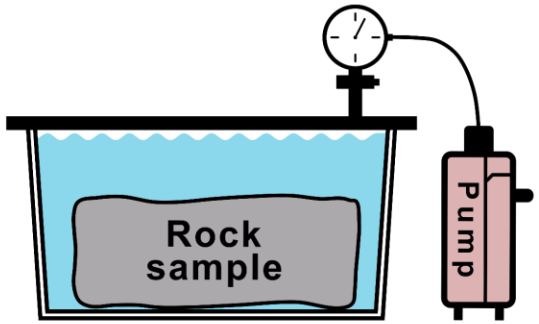

(3) Adhering medical gel electrodes

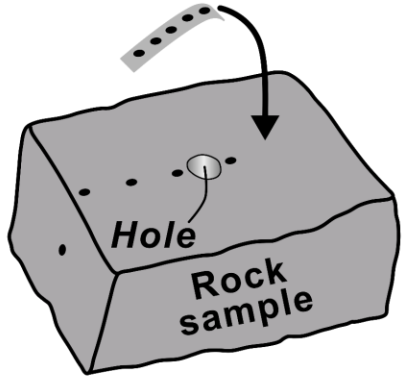

(4) Sample in climate chamber for SIP measurements

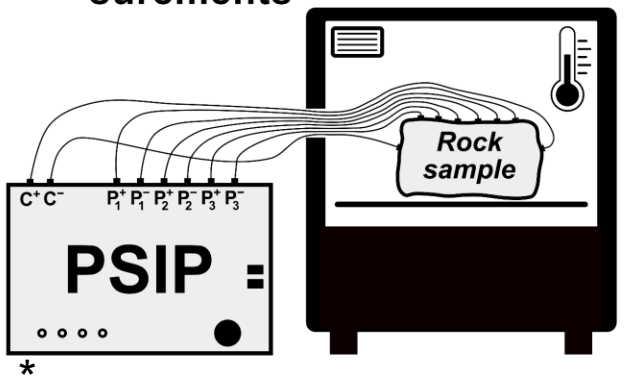

(5) SIP data collection with air-filled hole

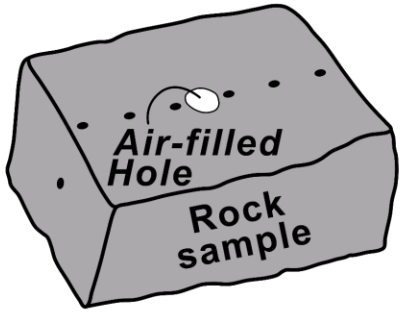

(6) Fill hole with water of certain σ_f

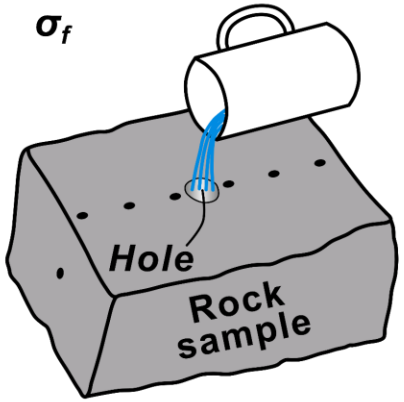

(7) Water in the hole freezes

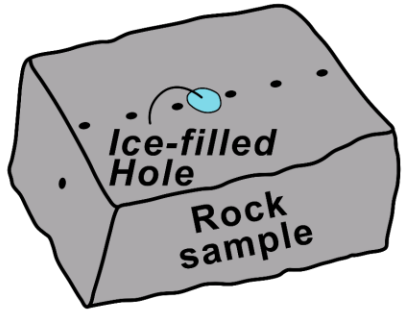

(8) SIP data collection with ice-filled hole

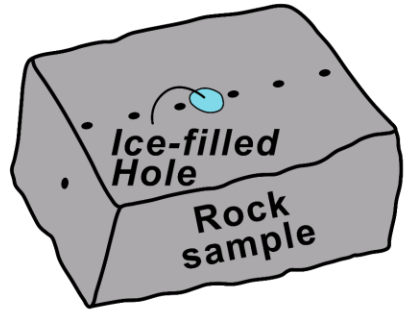

* Portable Field/Lab Spectral Induced Polarization (SIP) Unit (PSIP)

Rock samples

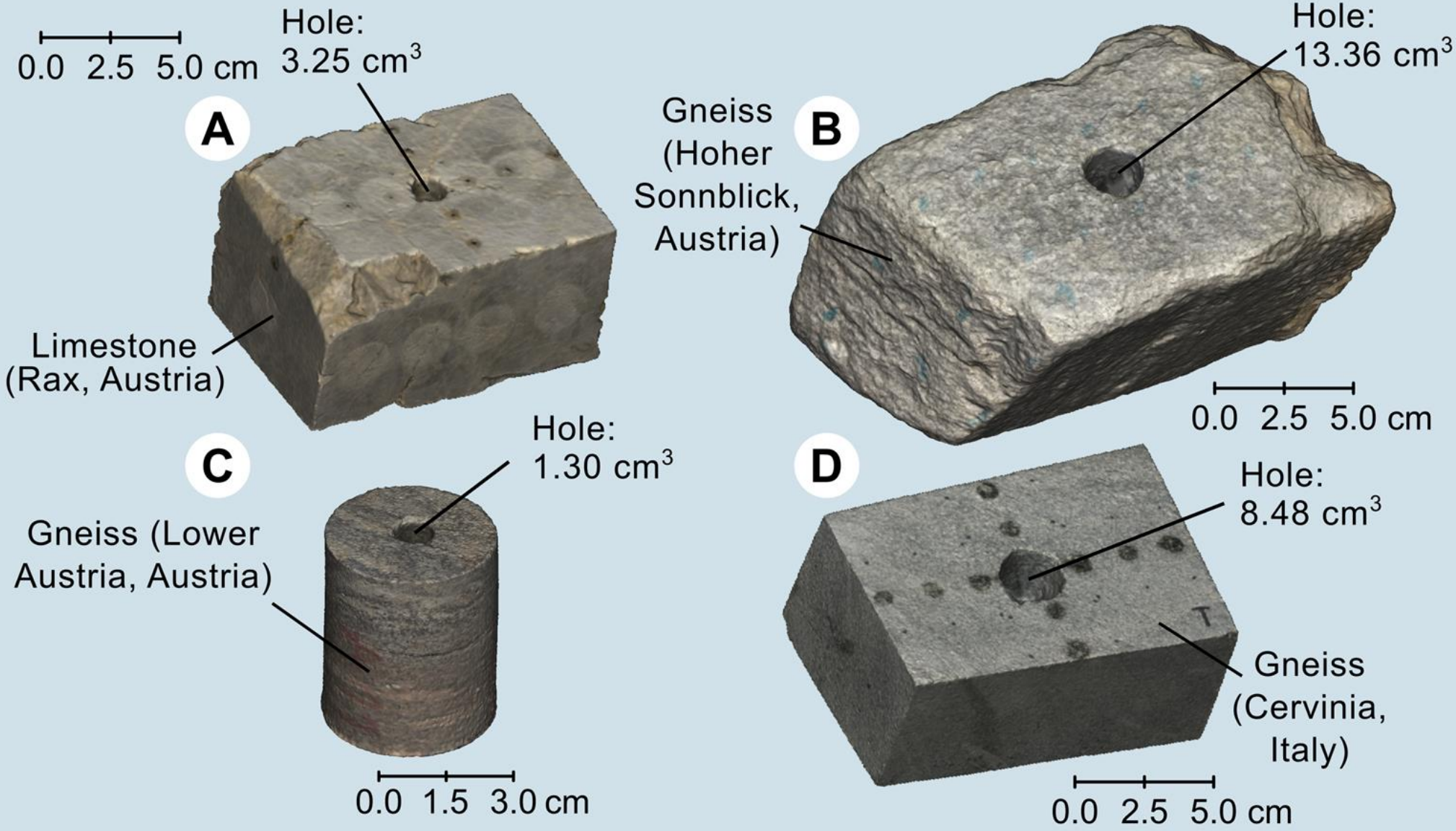

Polarization effects under thermal equilibrium

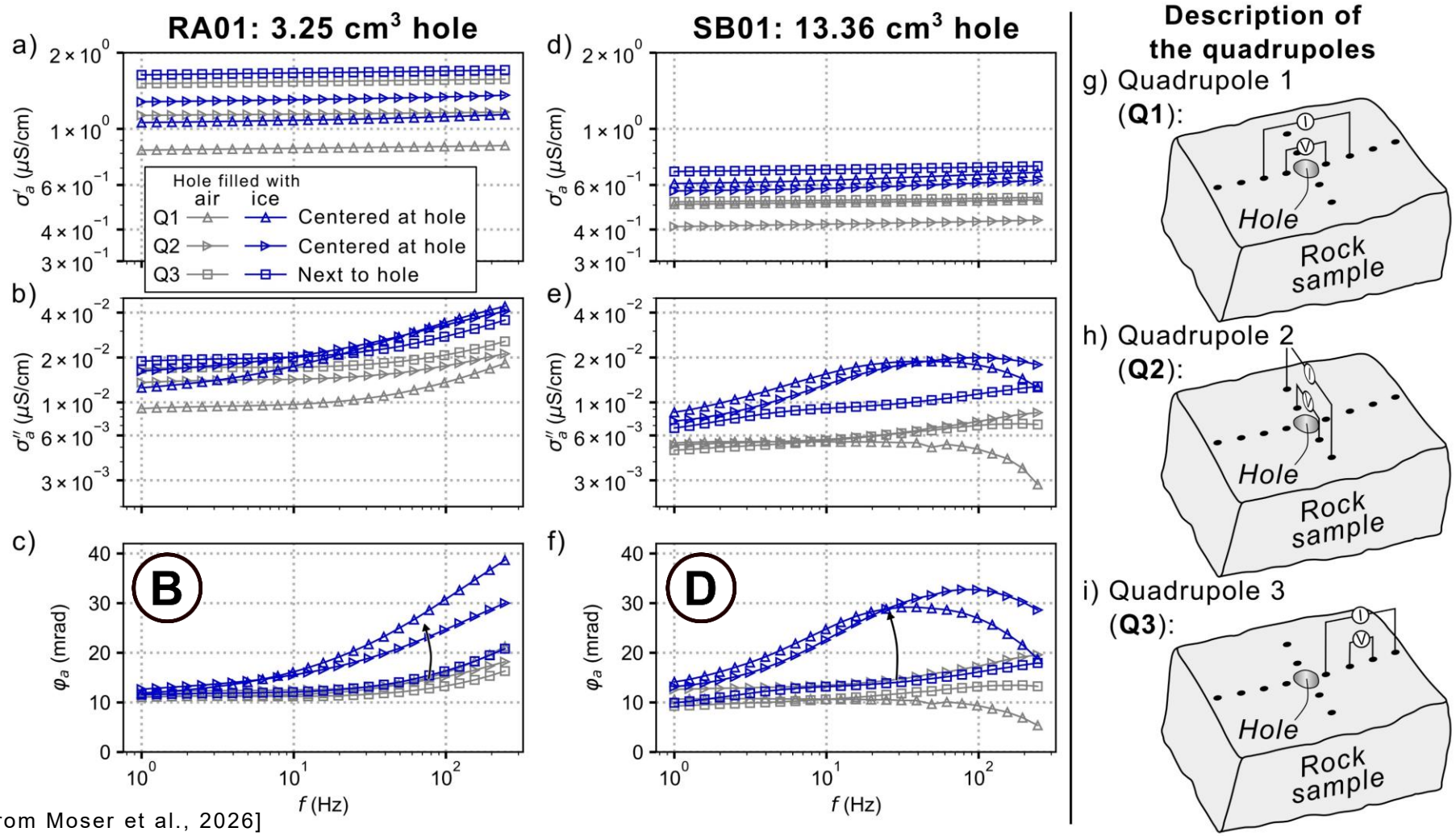

[Figure from Moser et al., 2026]

Polarization effects under thermal equilibrium

D Effect of varying hole diameter

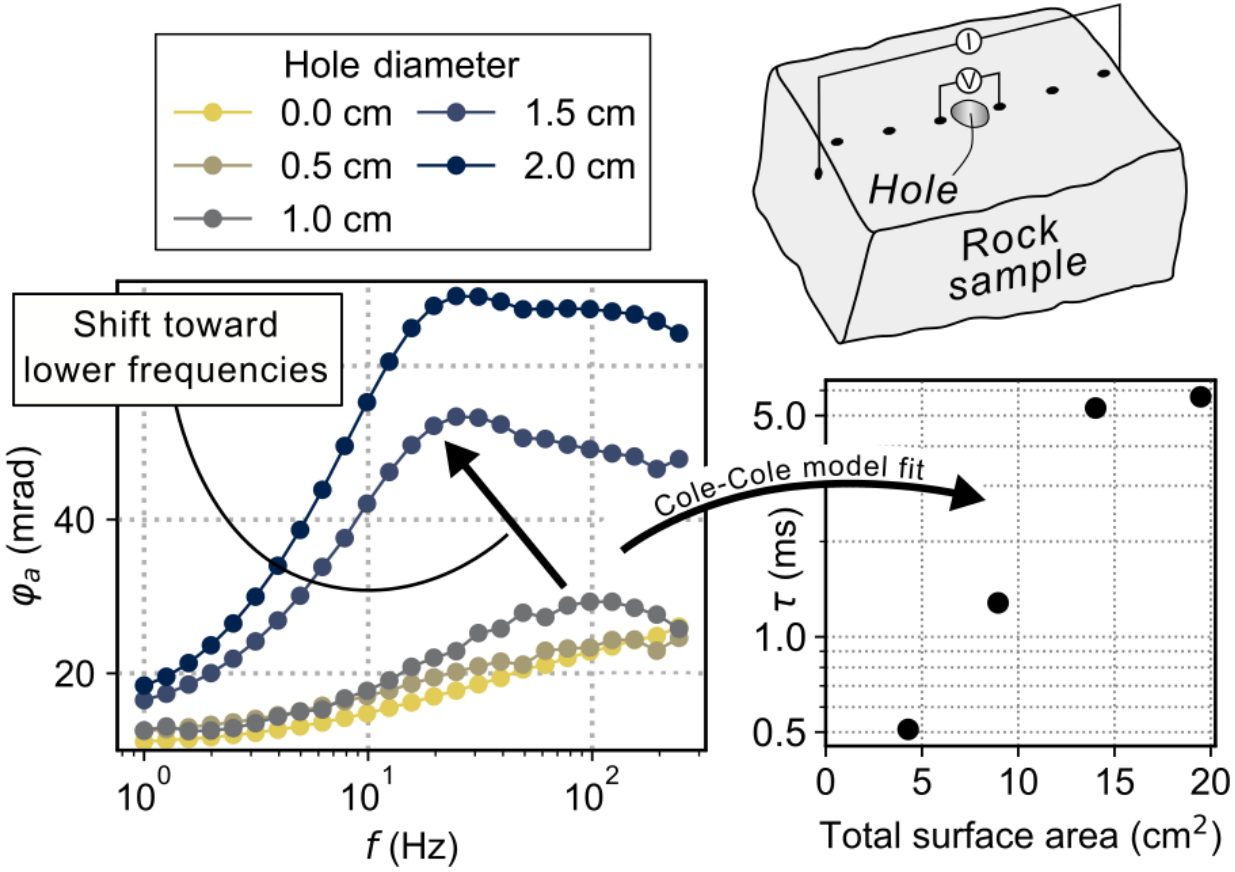

D Effect of varying salinity

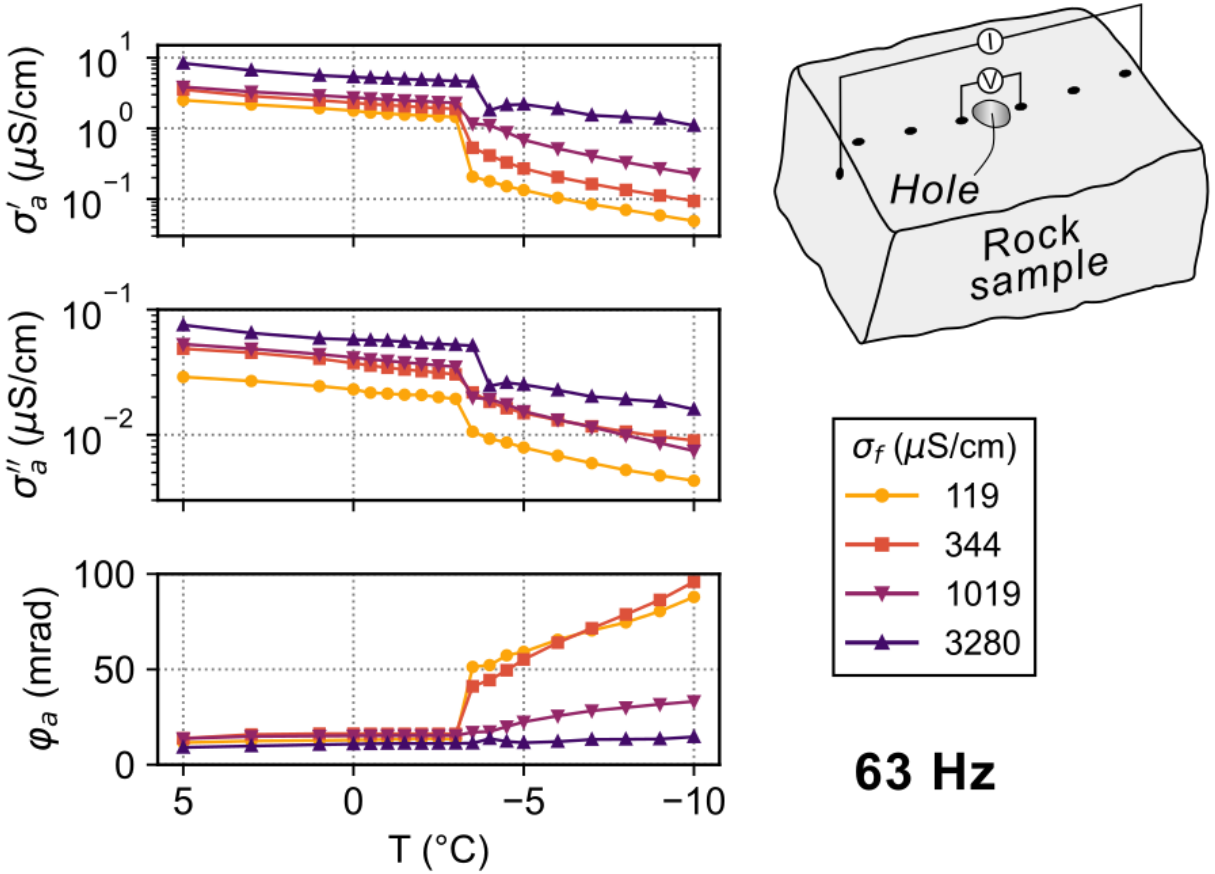

Polarization effects during ice formation

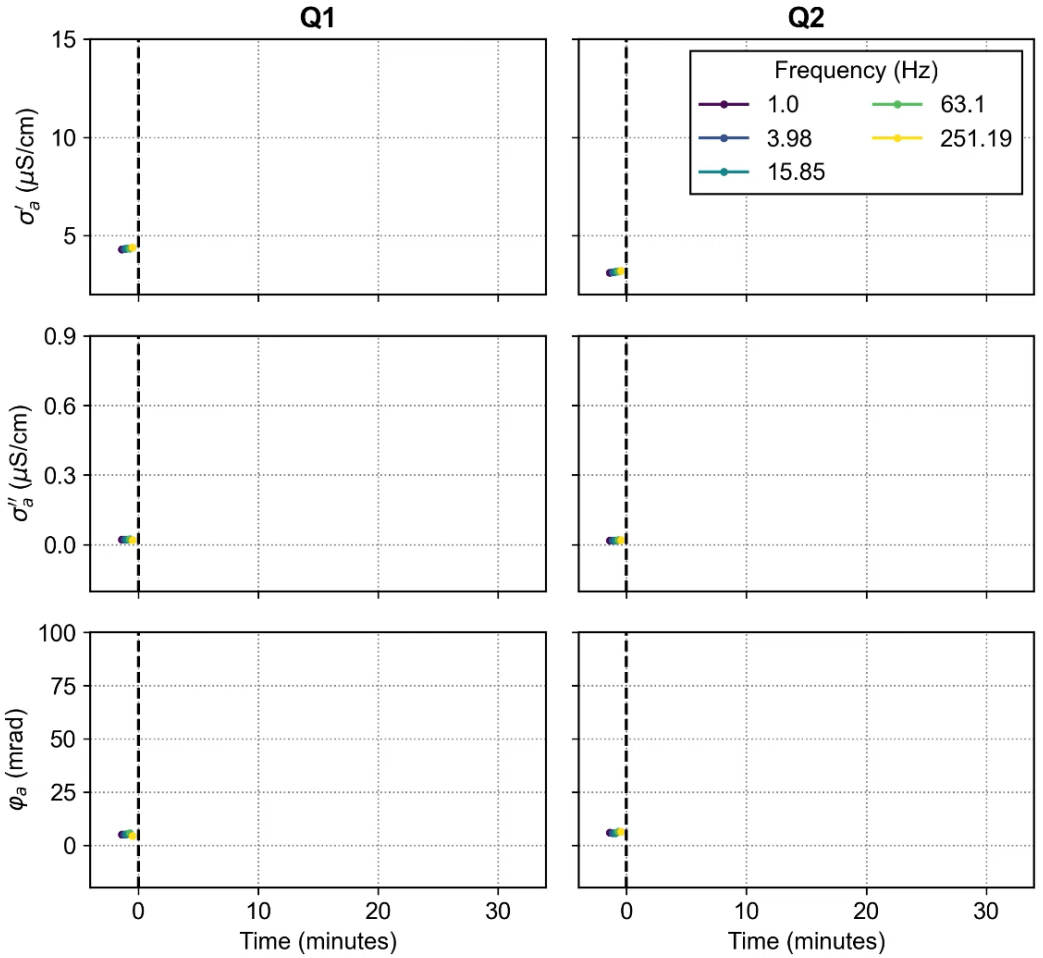

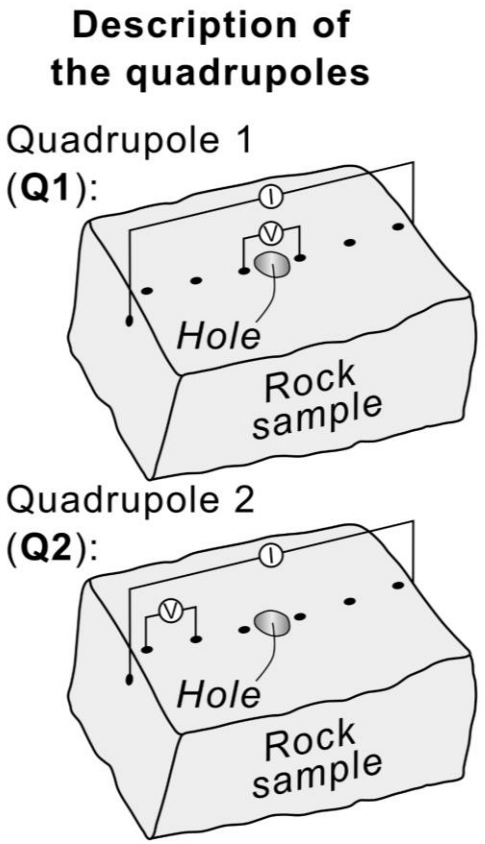

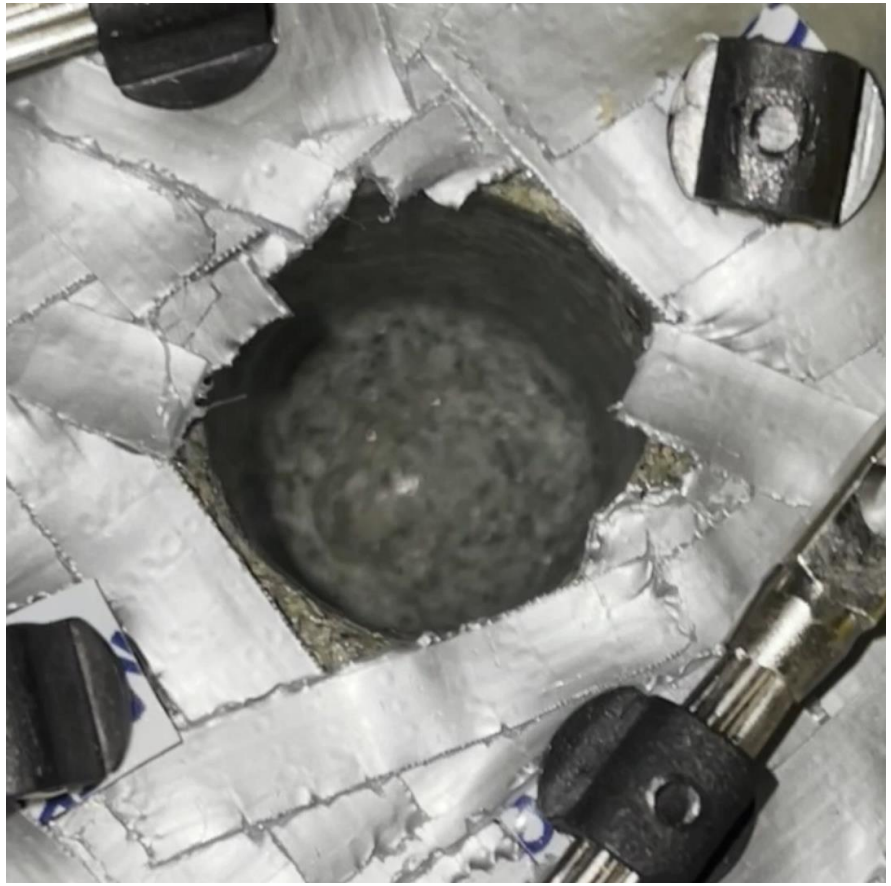

Sensitivity analysis

Quadrupole 1

Q1 is **positively (and highly) sensitive** to blank ice feature

Resistive and **polarizable** feature results in:

- Large $|\rho_a^*|$ increase
- φ_a increase (**positive IP effect**)

2 regions:

(1) Rock material:
ρ = 17000 Ωm; φ = -8 mrad

(1) Ice material (anomaly):
ρ = [10^2:10^6] Ωm; φ = [-200, -500, -800] mrad

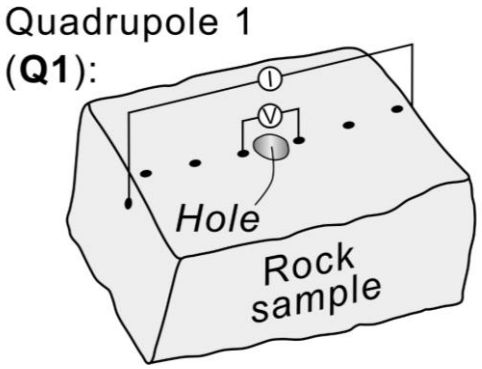

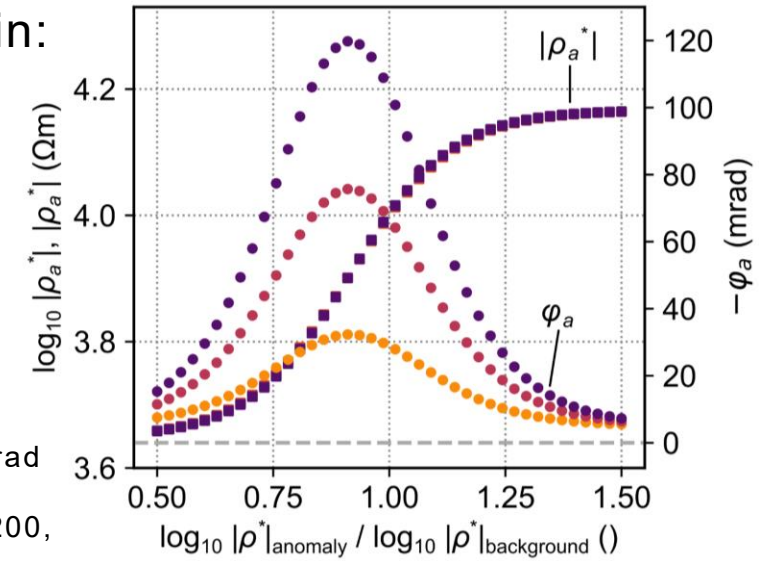

Quadrupole 2

Q2 is **negatively (and less) sensitive** to blank ice feature

Resistive and **polarizable** feature results in:

- Slight $|\rho_a^*|$ decrease
- φ_a decrease (**negative IP effect**)

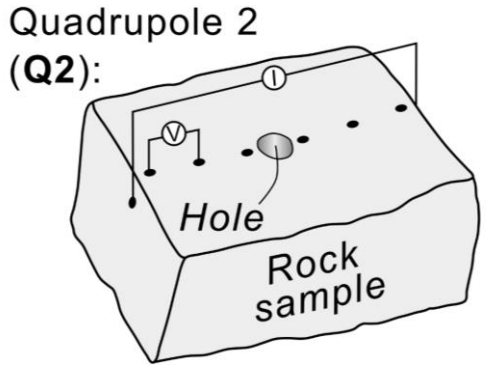

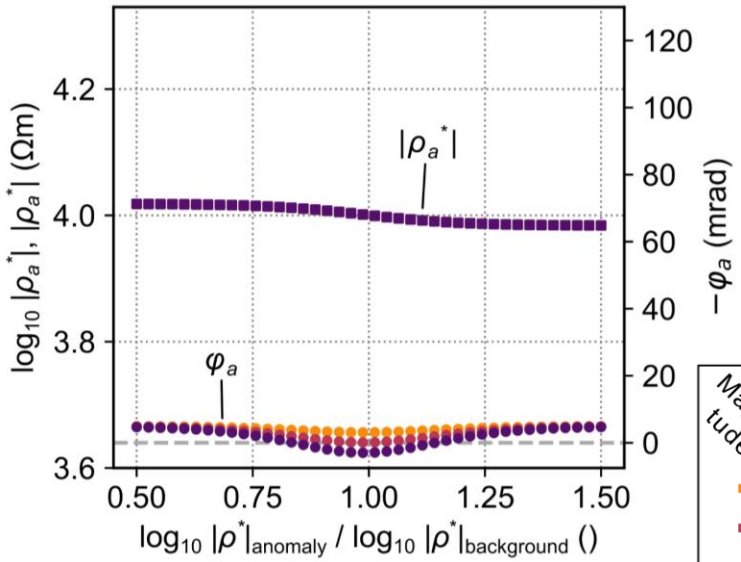

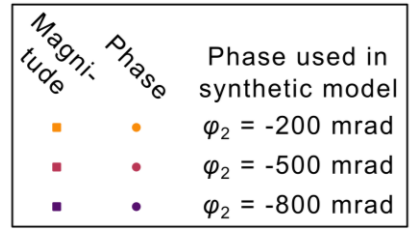

Polarization effects during ice formation

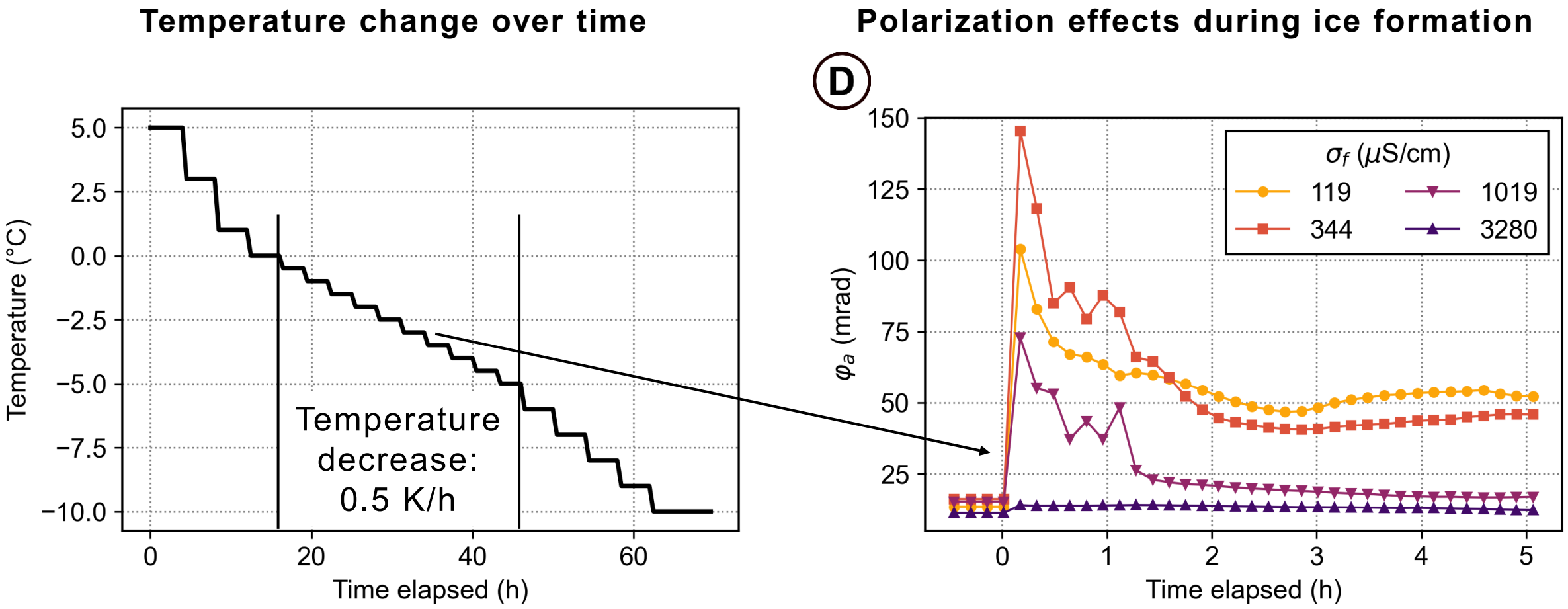

Imaging inversion results

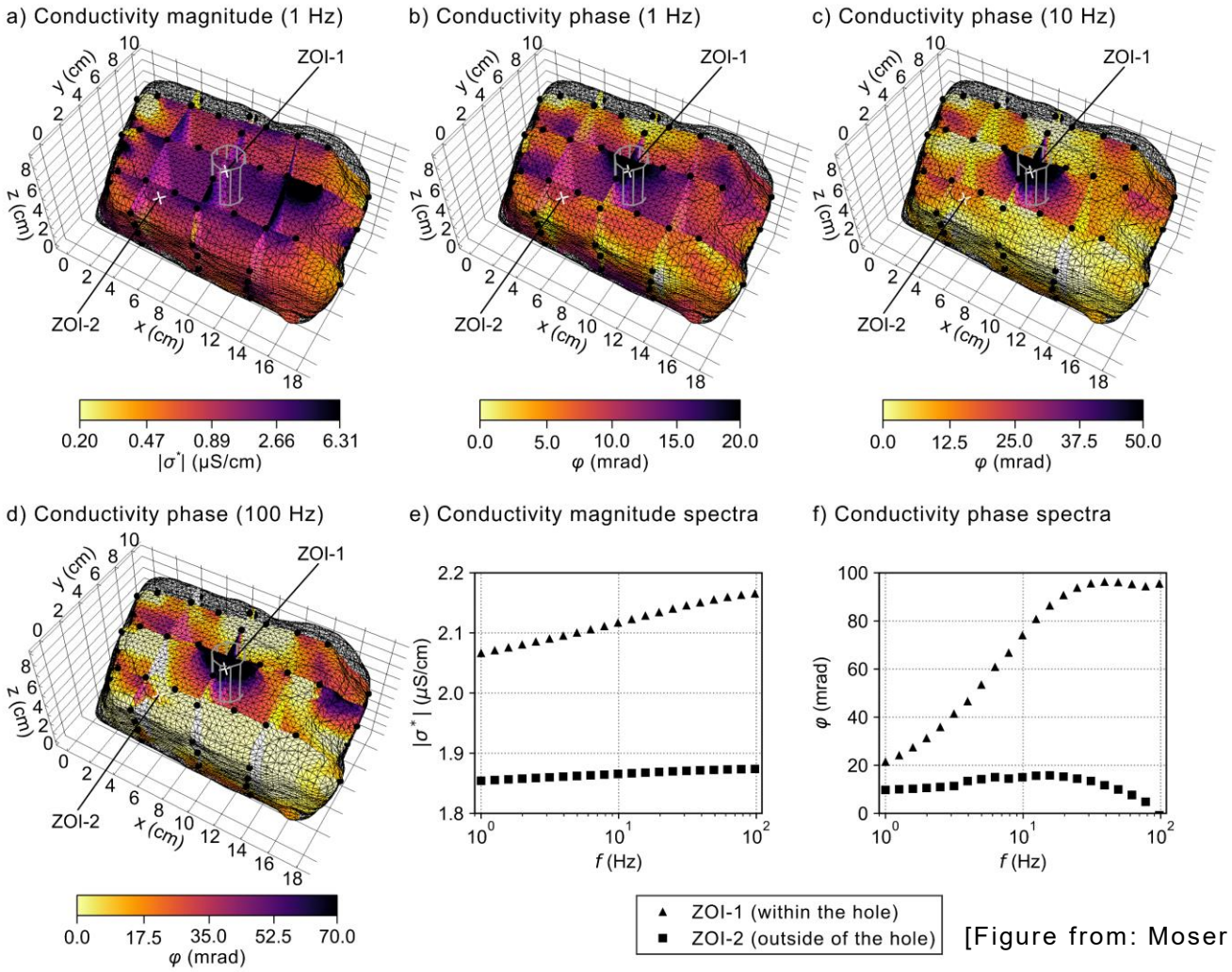

[Figure from: Moser et al., 2026]

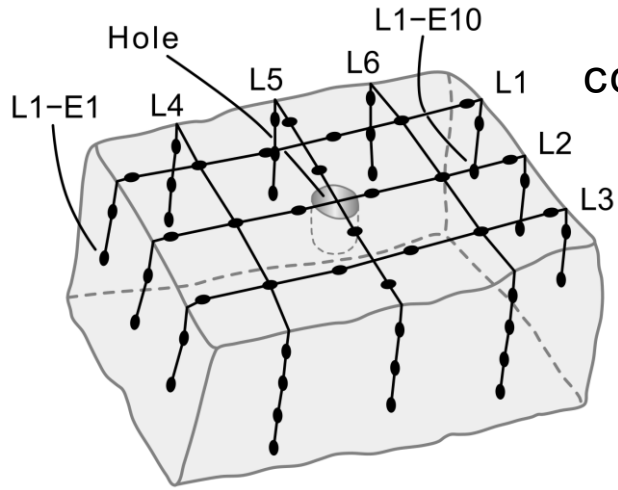

Electrode configuration

- **Conductivity magnitude:**
  - Almost no contrast between ice-filled hole and frozen rock material
- **Conductivity phase:**
  - Strong phase anomaly at position of ice-filled hole at f = 1–100 Hz

Imaging inversion results

CT scan

Vertical slice

Horizontal slice

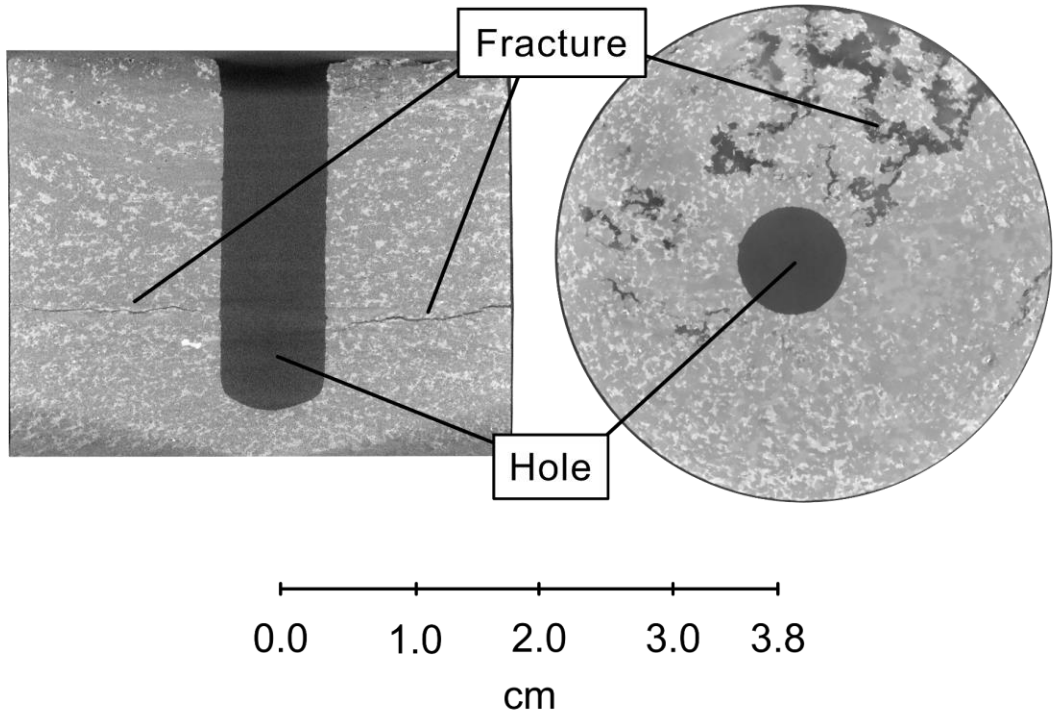

3D inversion result at 15 Hz

Ice-filled state

Difference between ice- and air-filled state

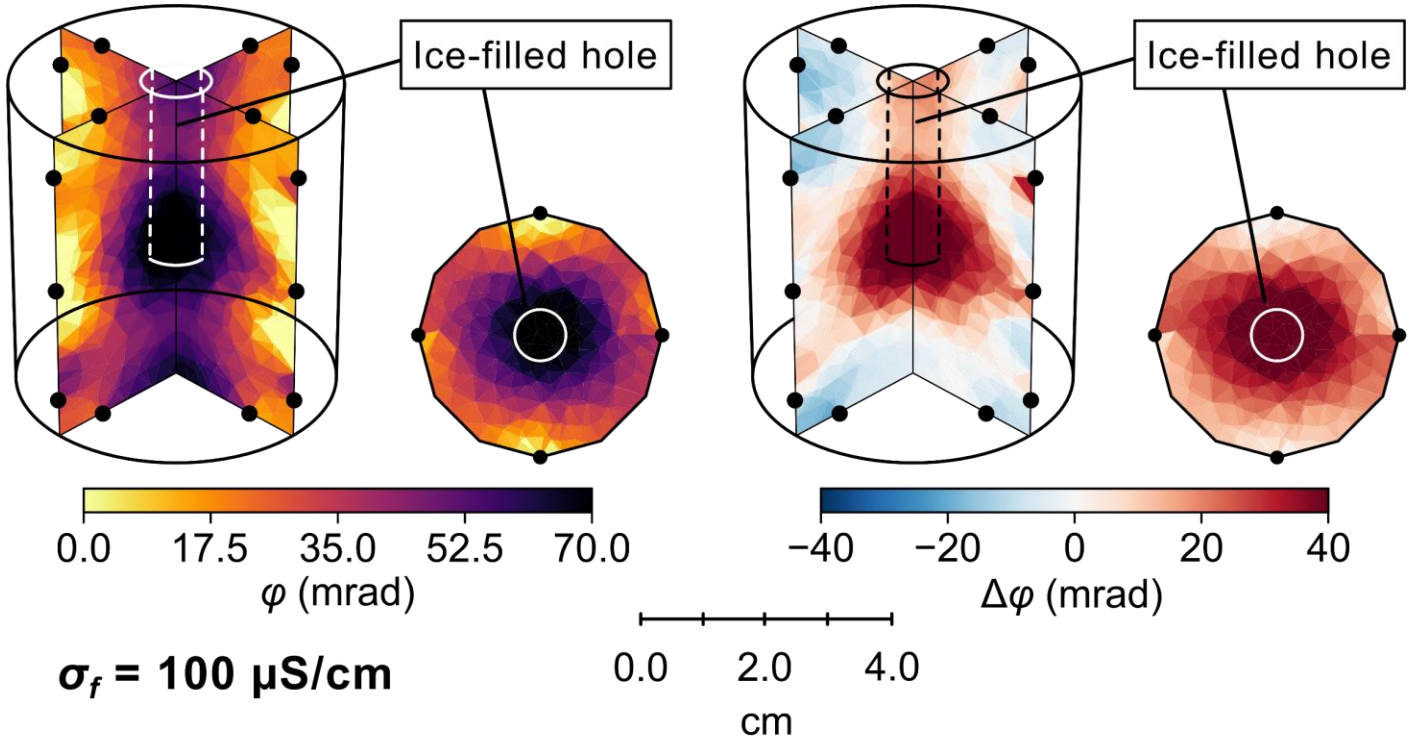

σ_f = 100 µS/cm

Conclusions experiment 1

1) **Blank ice features** in solid rock discontinuities **polarize** between 1–100 Hz in thermal equilibrium.

2) The polarization response **increases** with **increasing hole diameter**, and in turn, with increasing ice volume.

3) Even stronger **polarization effect during the formation of ice** due to charge separation between ice and liquid water (Workman-Reynolds-Freezing-Potential effect).

(2) Tank experiment

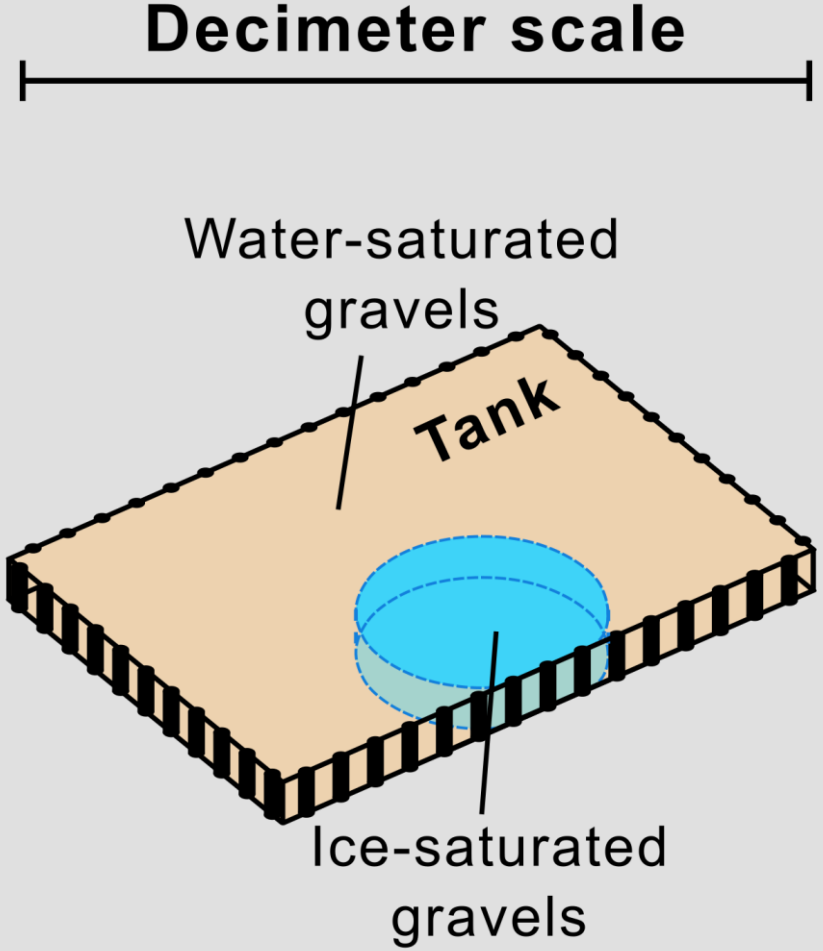

Experiment overview

Picture

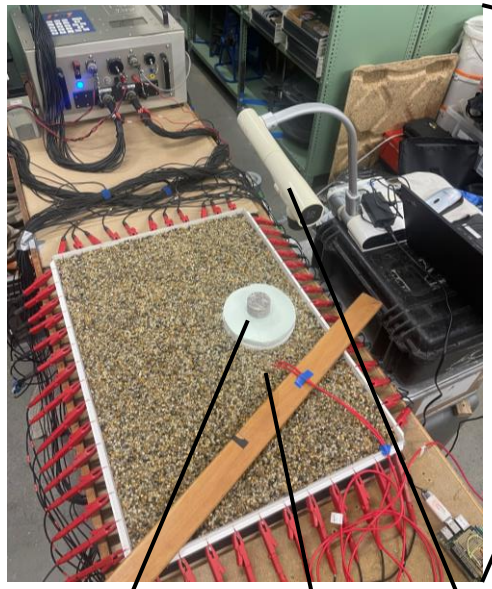

Sketch

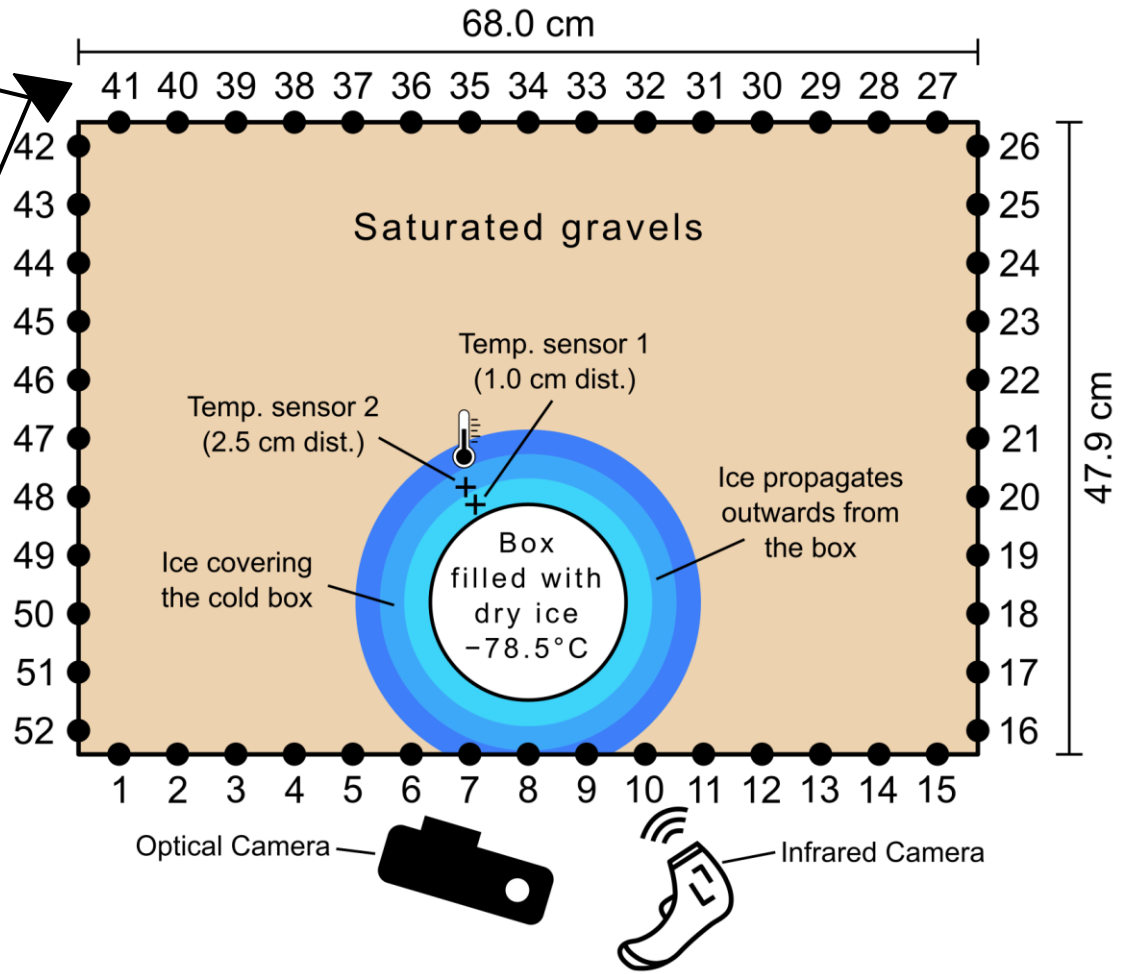

Experimental setup

- **Tank** dimensions: 68.0 × 47.9 × 3.0 cm
- **Box** with dry ice:
  - 15.0 cm diameter
  - 4.0 cm distance from tank edge
- **SIP** measurements:
  - 52 electrodes with 4.4 cm spacing
- **Temperature** sensors:
  - Sensor 1: 1.0 cm distance from box
  - Sensor 2: 2.5 cm distance from box
- **Optical camera**: Continuous video
- **Infrared camera**: Single shot at ice maximum

Porosity / Water content: 34.64 %
Fluid conductivity: ~330 µS/cm

Temperature

Temperature over time measured by temp. sensors

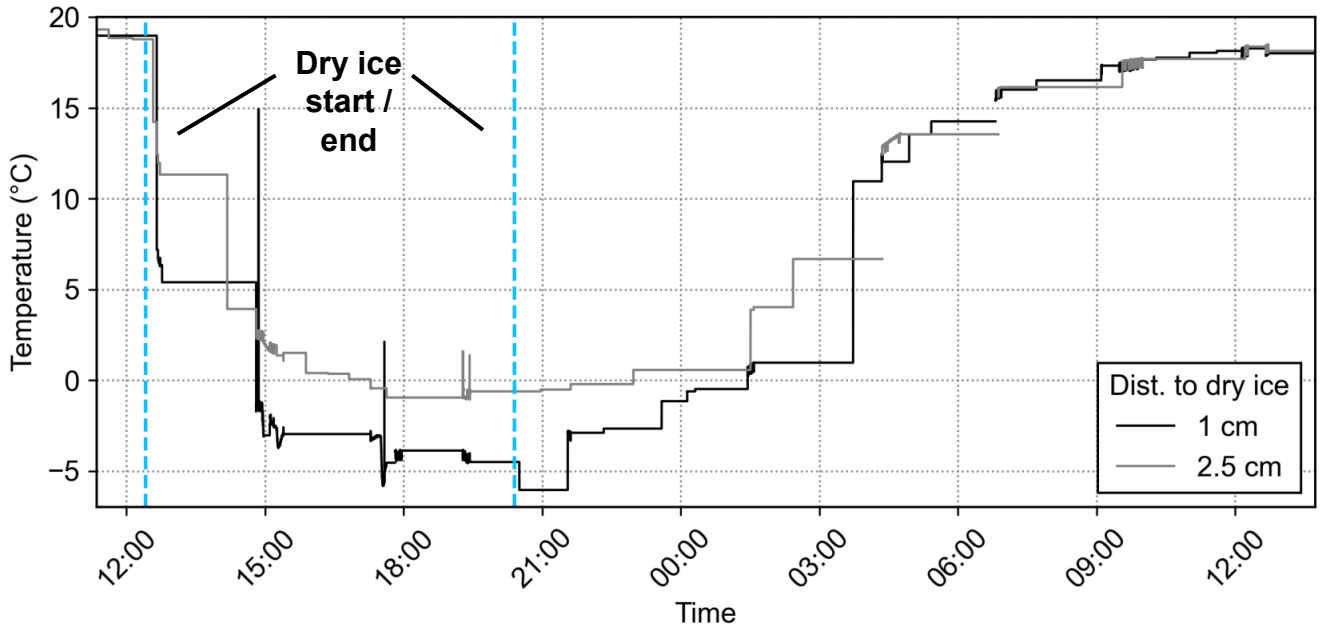

- **T < 0 °C**
  - 1 cm dist.: ~2.5 h after first dry ice, ~5 h after dry ice
  - 2.5 cm dist.: ~4.5 h after dry ice, ~3 h after last dry ice

Infrared pictures

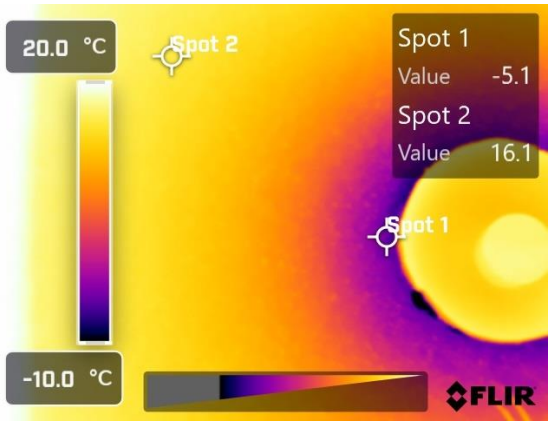

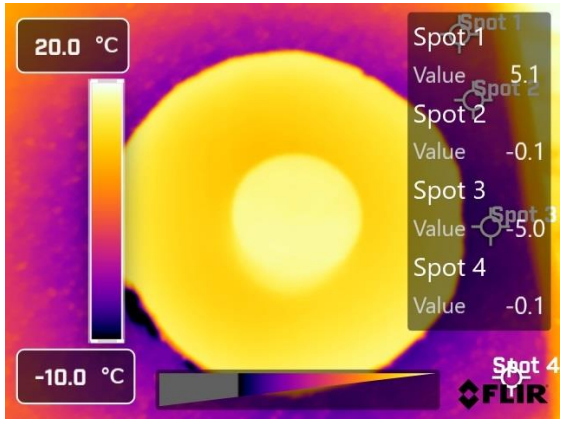

SIP data collection

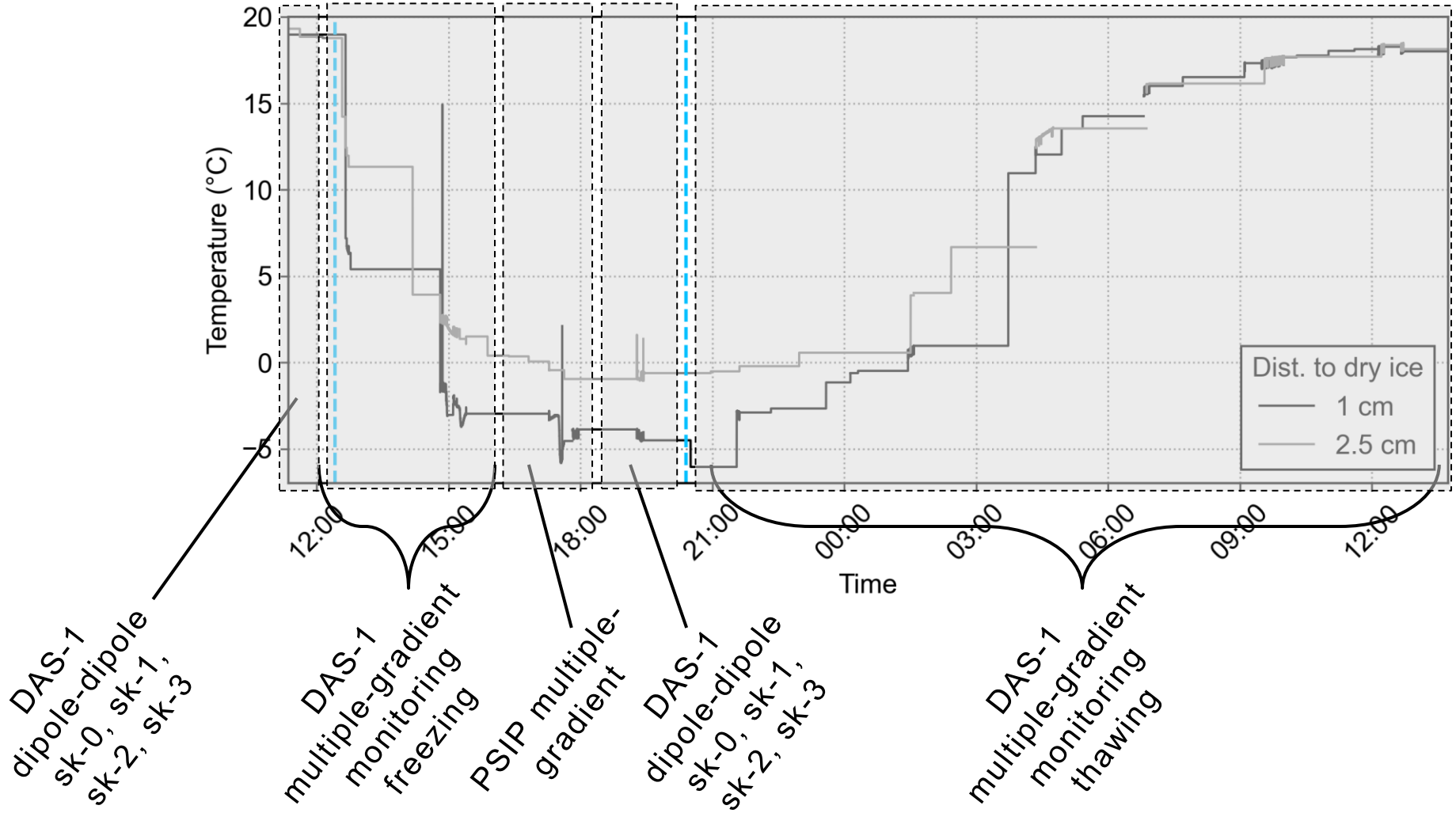

Numerical modeling

Electrode combinations tested

- Dipole-dipole (DD) sk-3 all levels
- Multiple-Gradient (MG)
- DD sk-0, DD sk-1, DD sk-2 only 8 levels

Data visualizations

Only inline data*:
Pseudoposition

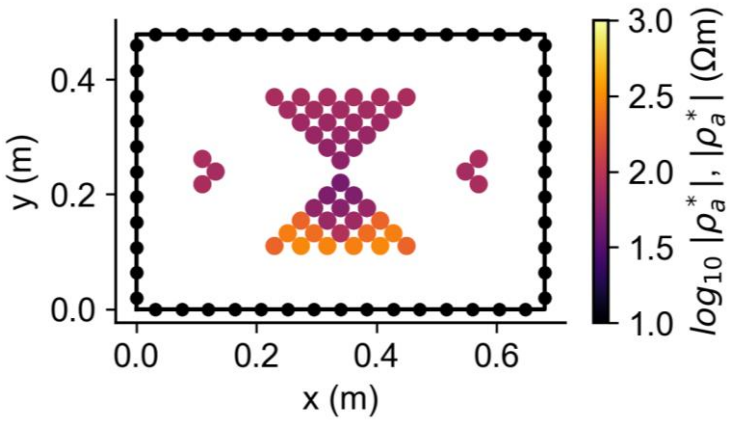

All data:
A vs. *M*

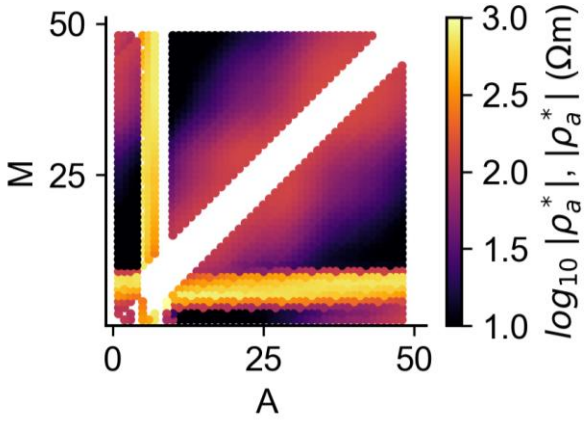

(2) Water-saturated gravels:
$|\rho^*| = 87.5$ Ωm
$\varphi = -0.5$ mrad

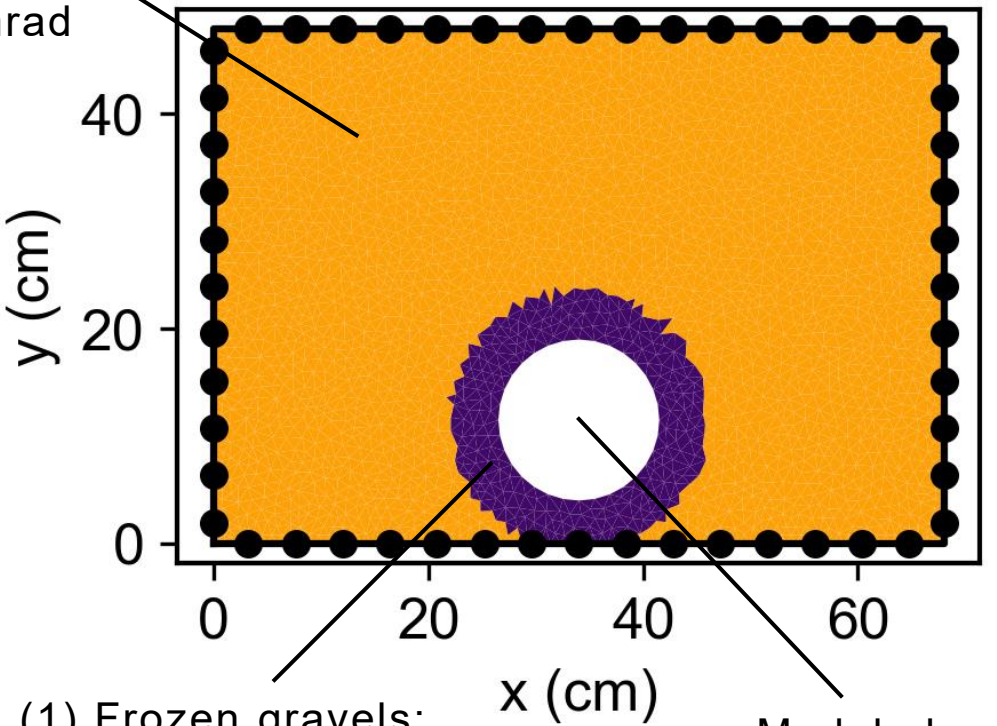

(1) Frozen gravels:
$|\rho^*| = 1000$ Ωm
$\varphi = -50.0$ mrad

Modeled as a hole

*Quadrupoles with all electrodes A,B,M,N along one edge of the box

DD sk-3: Measured vs. modeled data

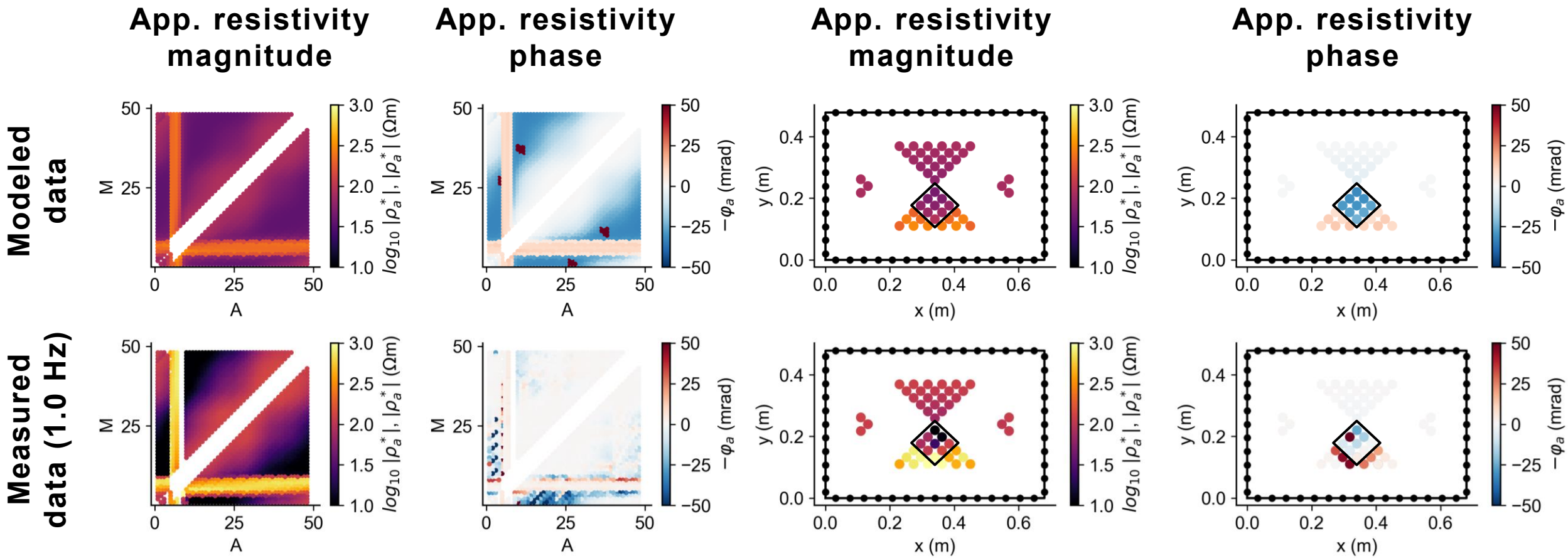

DD sk-0: Measured vs. modeled data

All data

App. resistivity magnitude

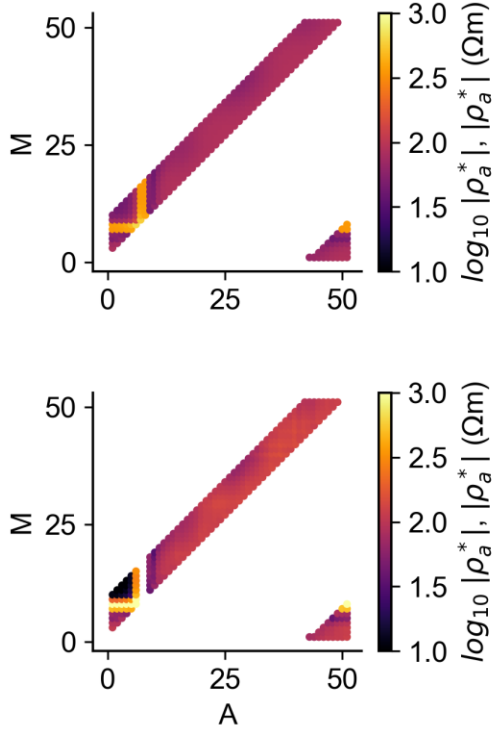

App. resistivity phase

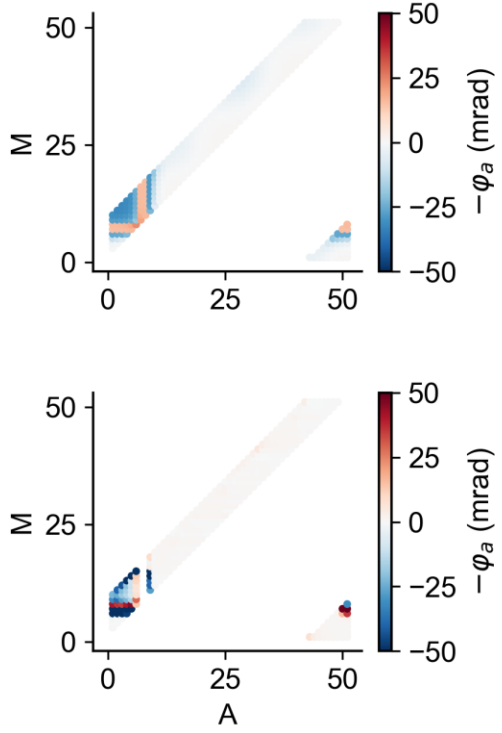

Only inline data

App. resistivity magnitude

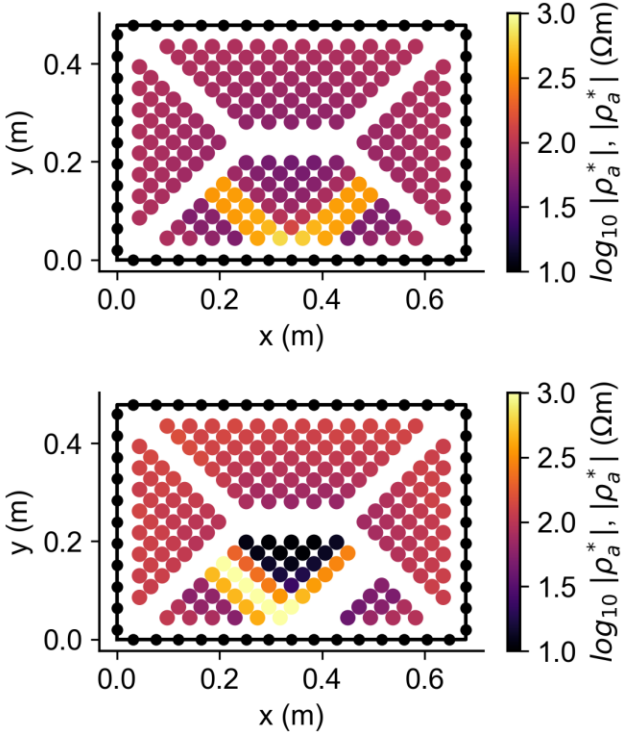

App. resistivity phase

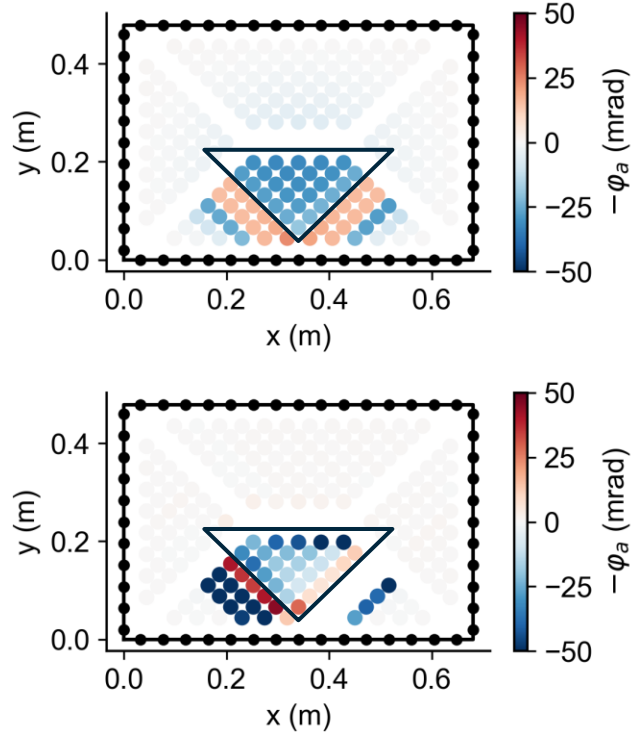

MG: Measured vs. modeled data

All data

App. resistivity magnitude

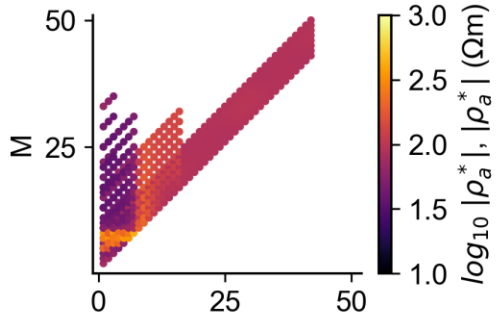

App. resistivity phase

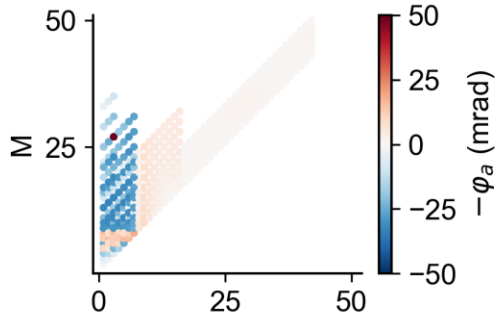

Only inline data

App. resistivity magnitude

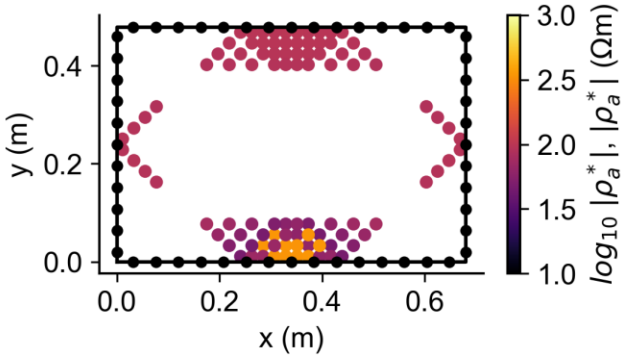

App. resistivity phase

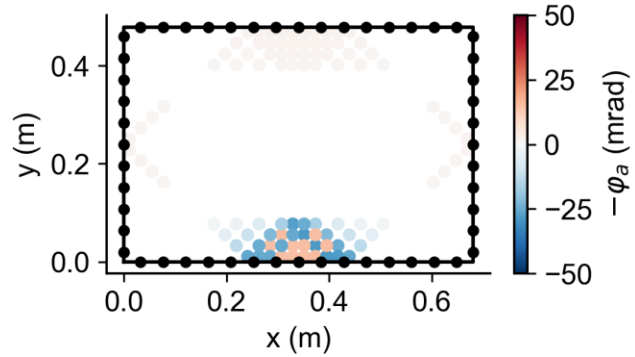

Time-lapse inversion results

t0: 2026-03-25 12:02:27

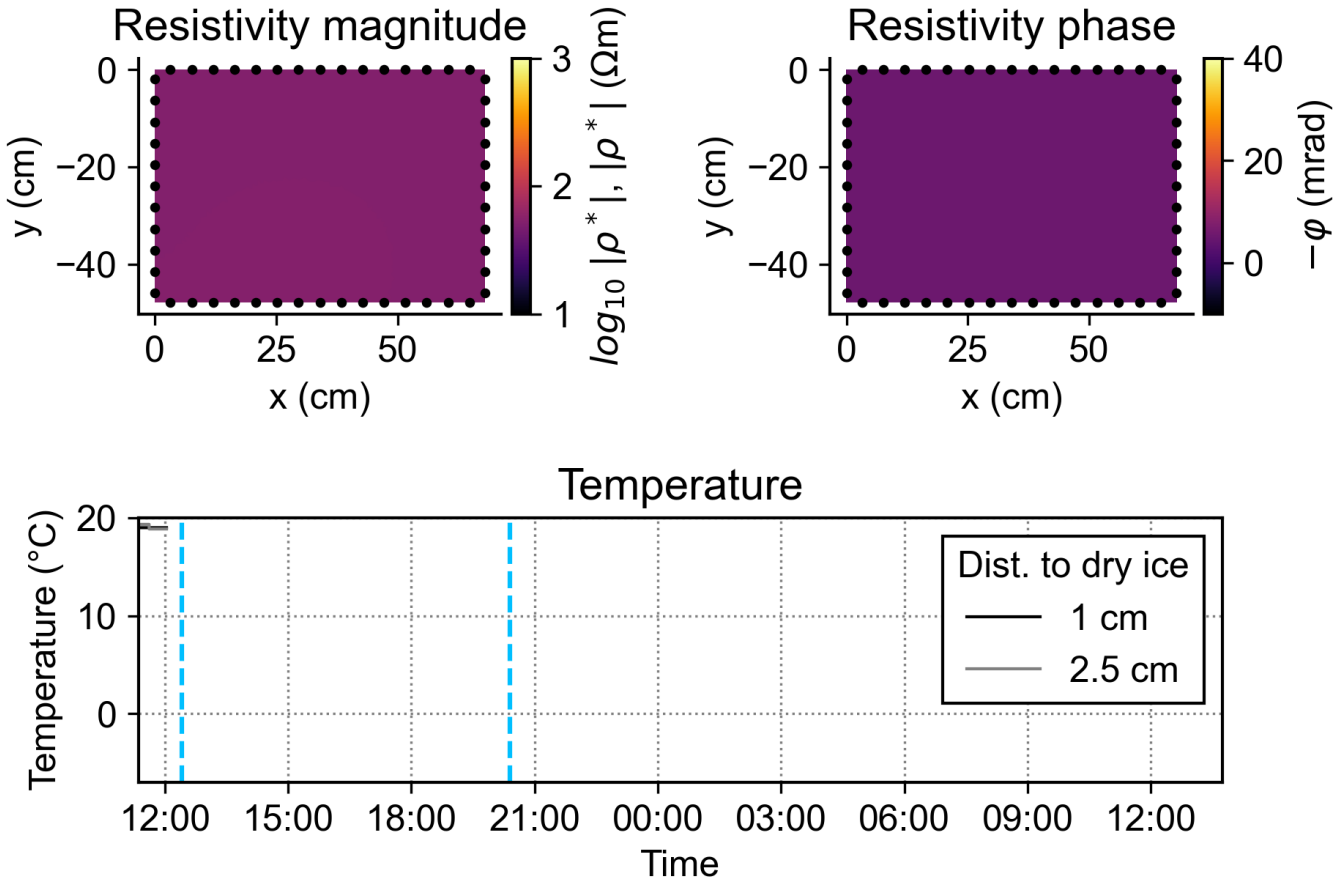

Frequency: 7.5 Hz

Preliminary observations:

- **Period 1 (without ice):** Low contrast in $|\rho^*|$ and φ between water-saturated gravels and resistive air-filled box
- **Period 2 (freezing process):** Increasing $|\rho^*|$ and φ in ice-saturated anomaly
- **Period 3 (thawing):** Decreasing $|\rho^*|$ and φ during thawing

Time-lapse inversion results

t0: 2026-03-25 12:02:27

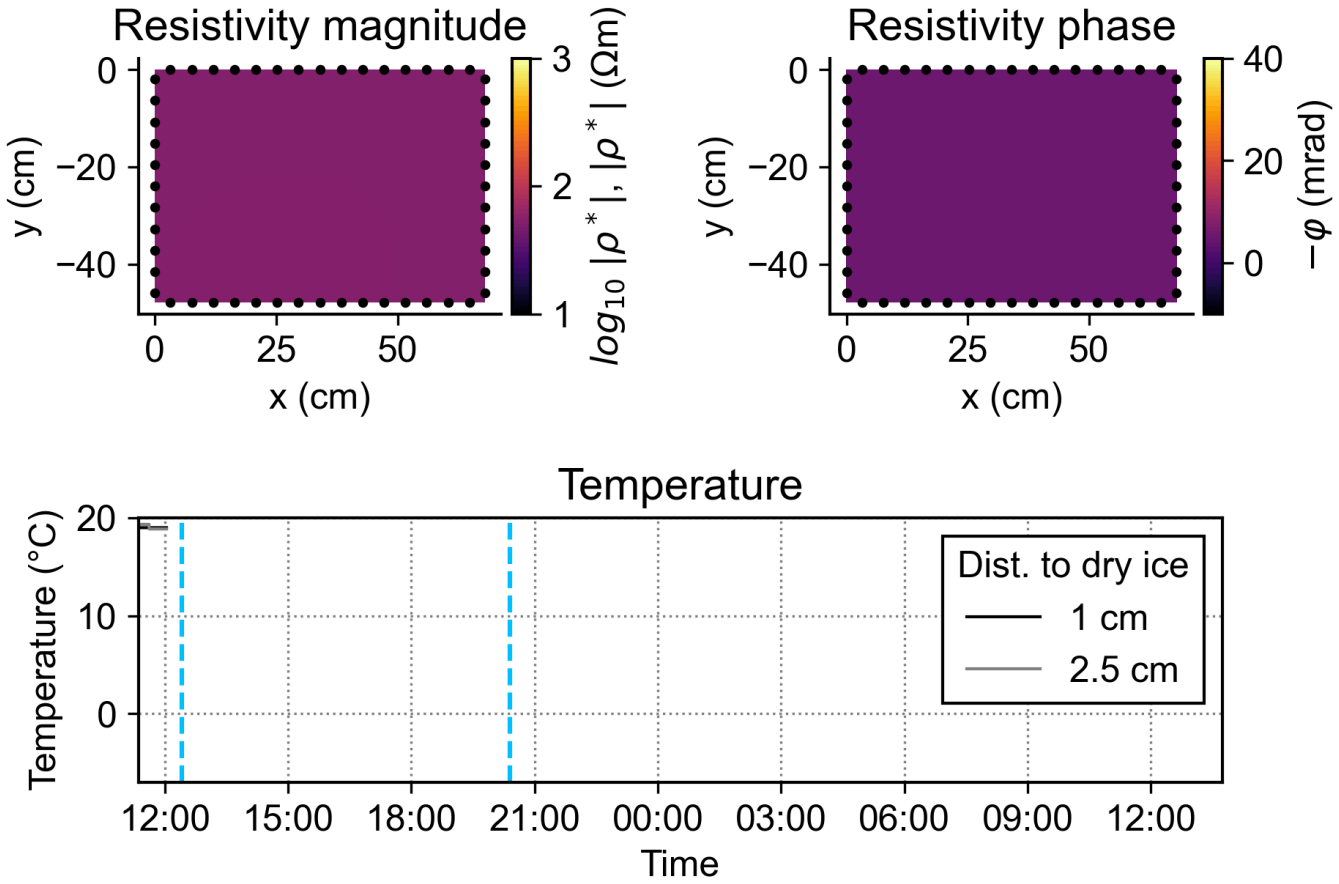

Frequency: 7.5 Hz

Preliminary observations:

- **Period 1 (without ice):** Low contrast in $|\rho^*|$ and φ between water-saturated gravels and resistive air-filled box
- **Period 2 (freezing process):** Increasing $|\rho^*|$ and φ in ice-saturated anomaly
- **Period 3 (thawing):** Decreasing $|\rho^*|$ and φ during thawing

PSIP profiling

Configuration

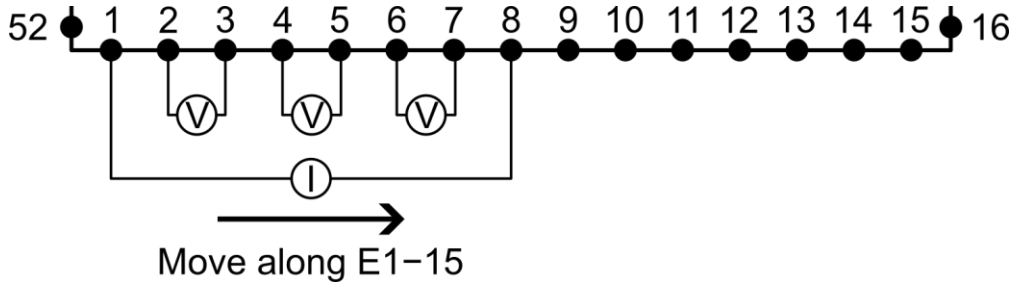

Symbology

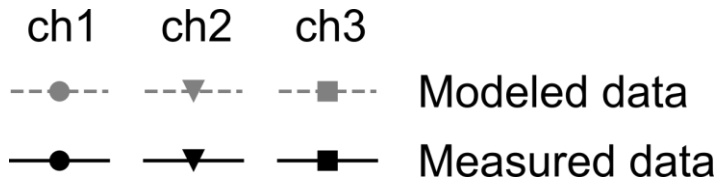

Results

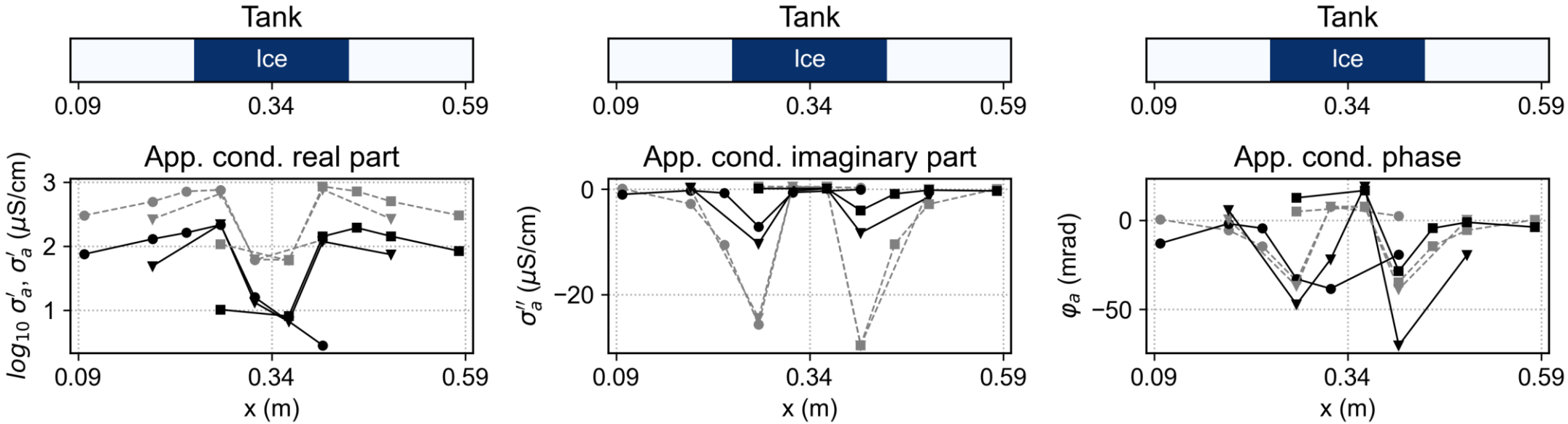

Conclusions experiment 2

1) **Low-frequency (1–100 Hz) polarization** effects can be also observed in **frozen sediments**

2) Frozen sediments act as a **resistive and polarizable anomaly**, which can result in **negative IP effects**

(1) Borehole experiment

Meter scale

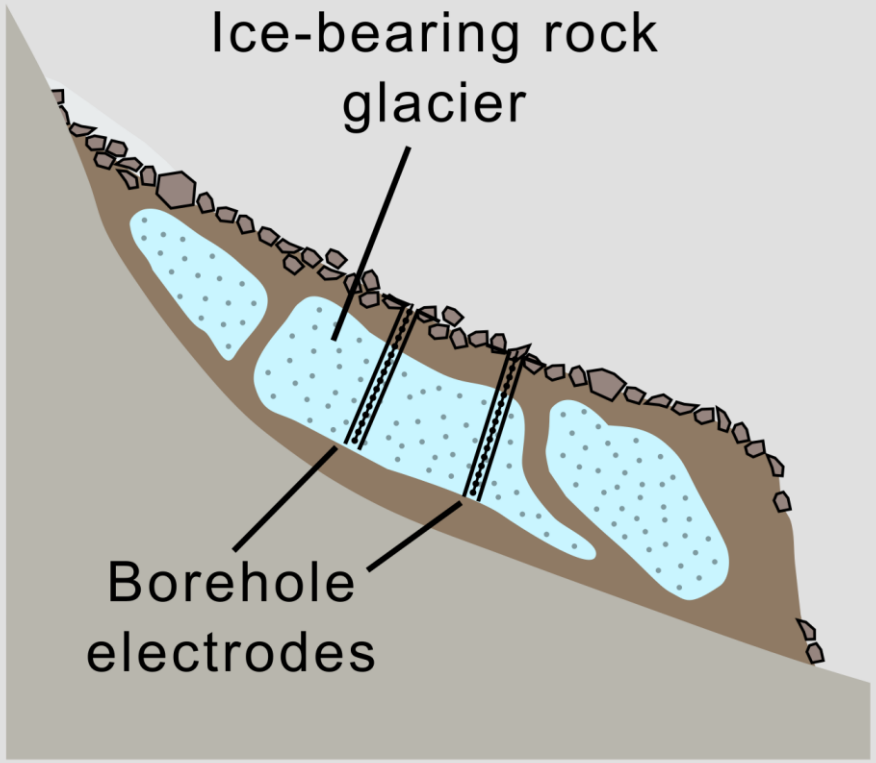

Study area: Rock glacier Muragl

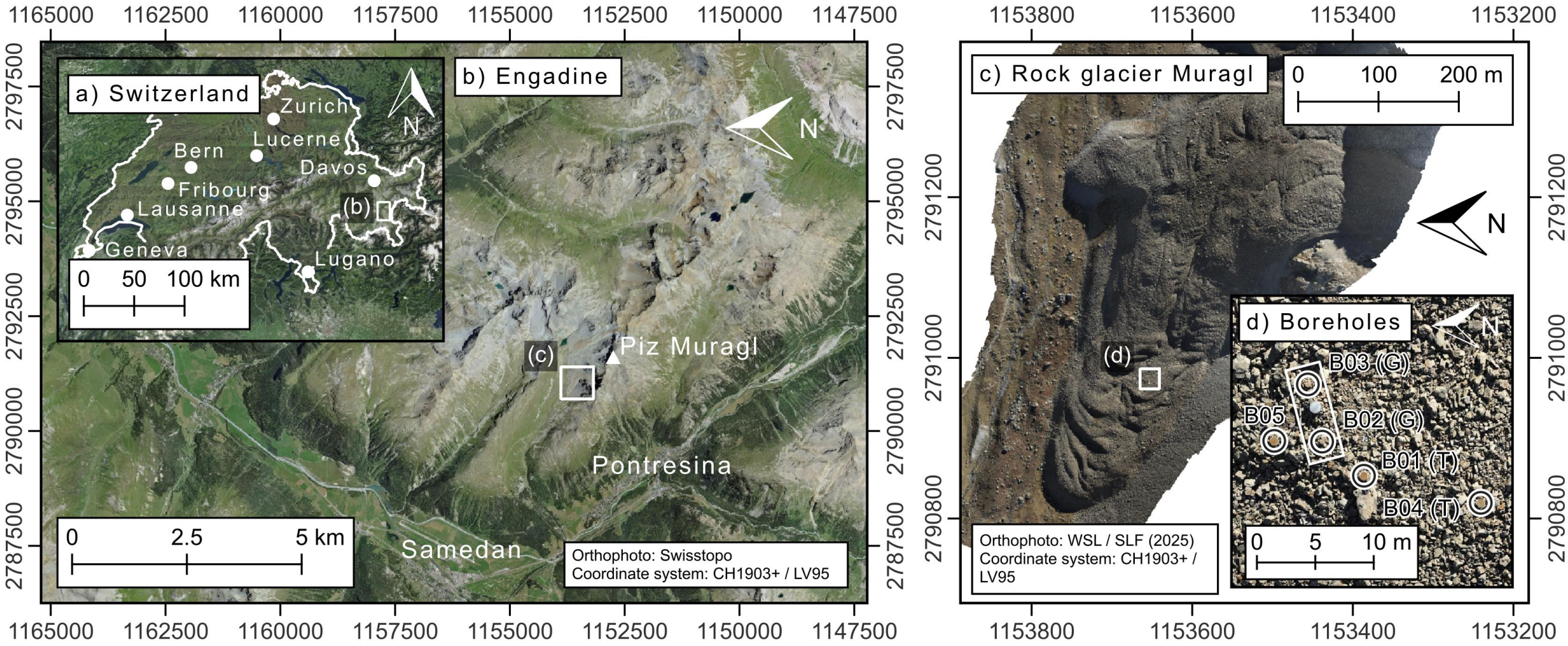

Borehole temperatures

Oct. 2024 – Oct. 2025

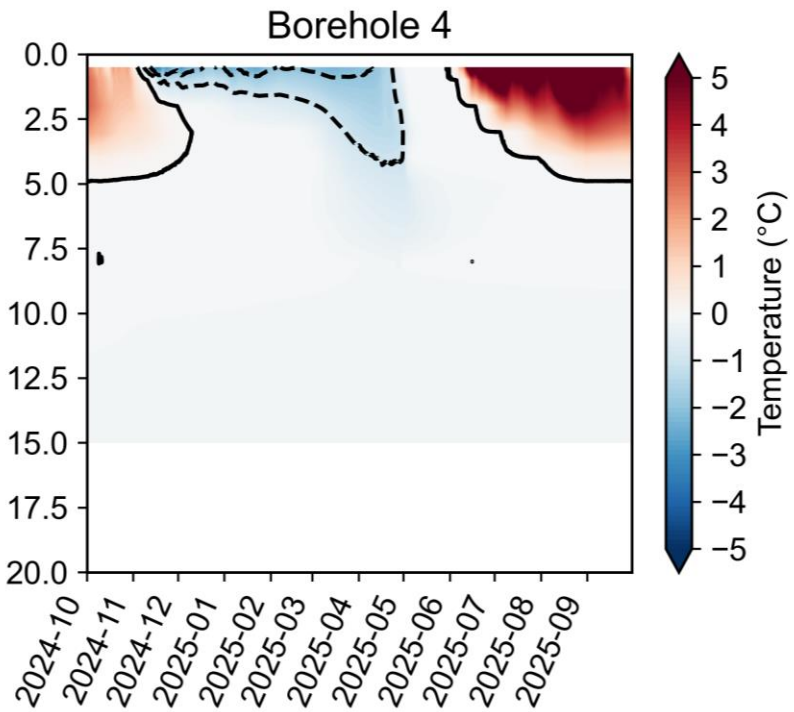

Aug. 2025 (During SIP data collection)

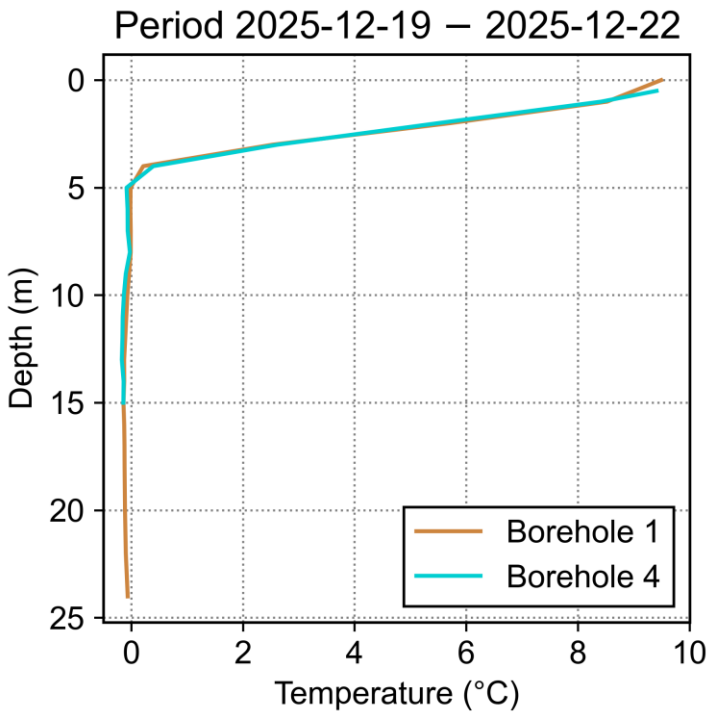

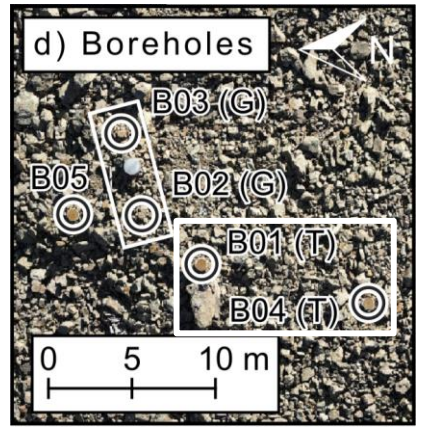

- **Active layer depth**: ~ 5 m
- **Permafrost**: ~ –0.1 °C, close to melting point

[Data from SLF (RoDynAlpS) & Permos (Swiss Permafrost Monitoring Network)]

Boreholes for SIP measurements

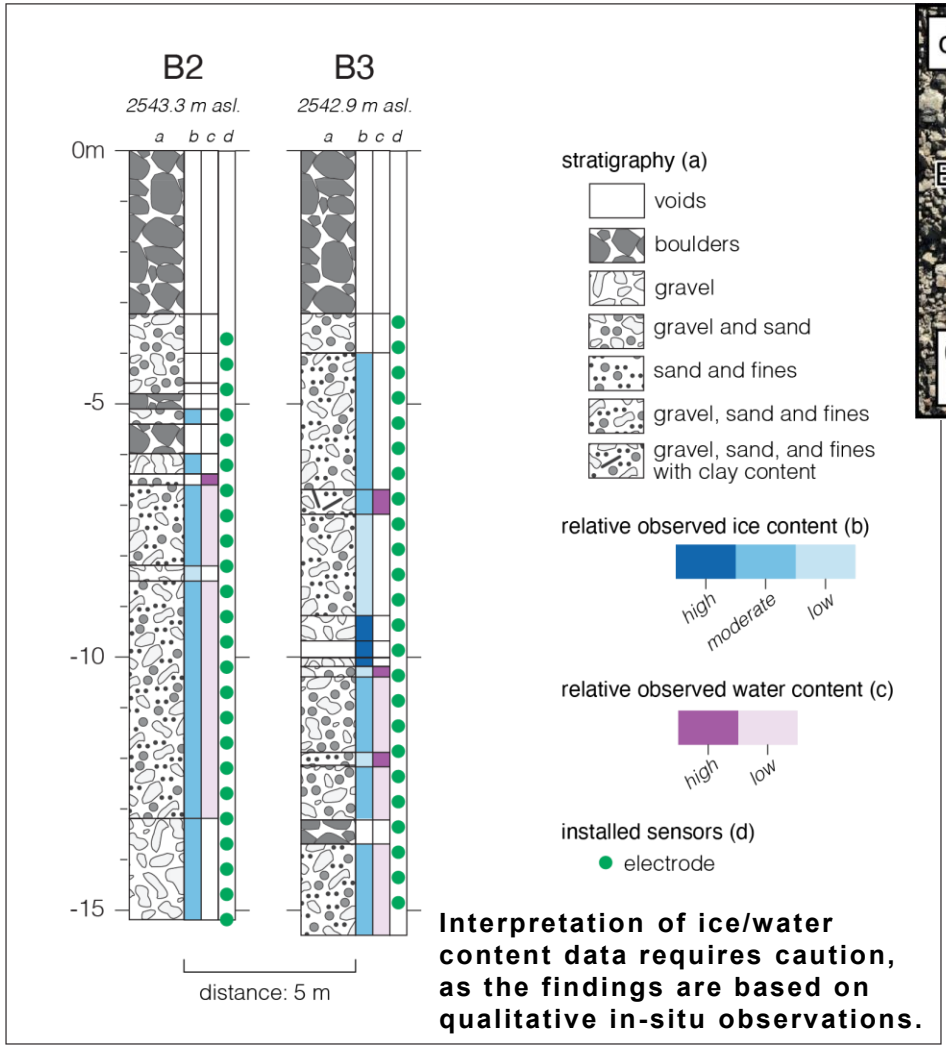

Interpretation of ice/water content data requires caution, as the findings are based on qualitative in-situ observations.

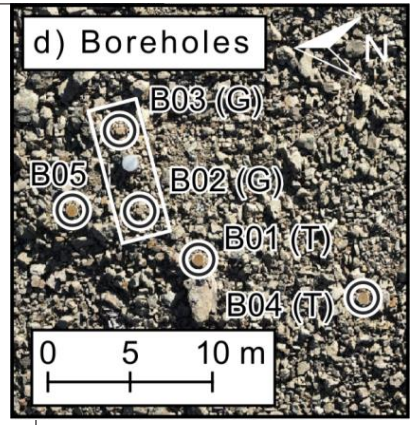

Borehole setup:

- Borehole depth: ~ 15 m
- Borehole distance: 5 m
- Electrode spacing: 0.5 m
- Electrodes per borehole: 24

SIP data collection

DAS-1 (field instrument)

- Dipole-Dipole sk-0 & sk-3 inline & cross-borehole
- Multiple-Gradient

→ Focus: Imaging

PSIP (lab instrument)

- Multiple-Gradient

→ Focus: Spectra over large frequency range

Contact resistances

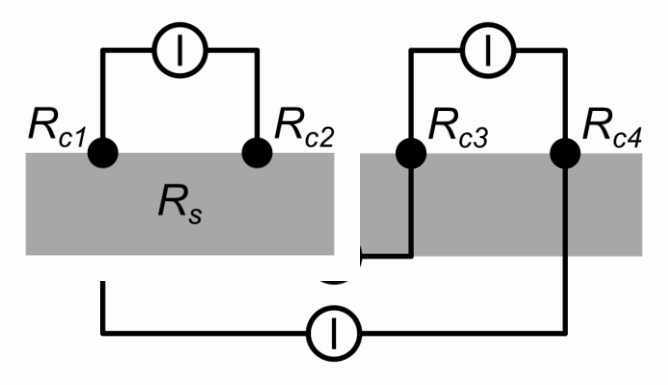

Measured:

$$R_g = R_{c1} + R_{c2} + R_s$$

... along several electrode combinations

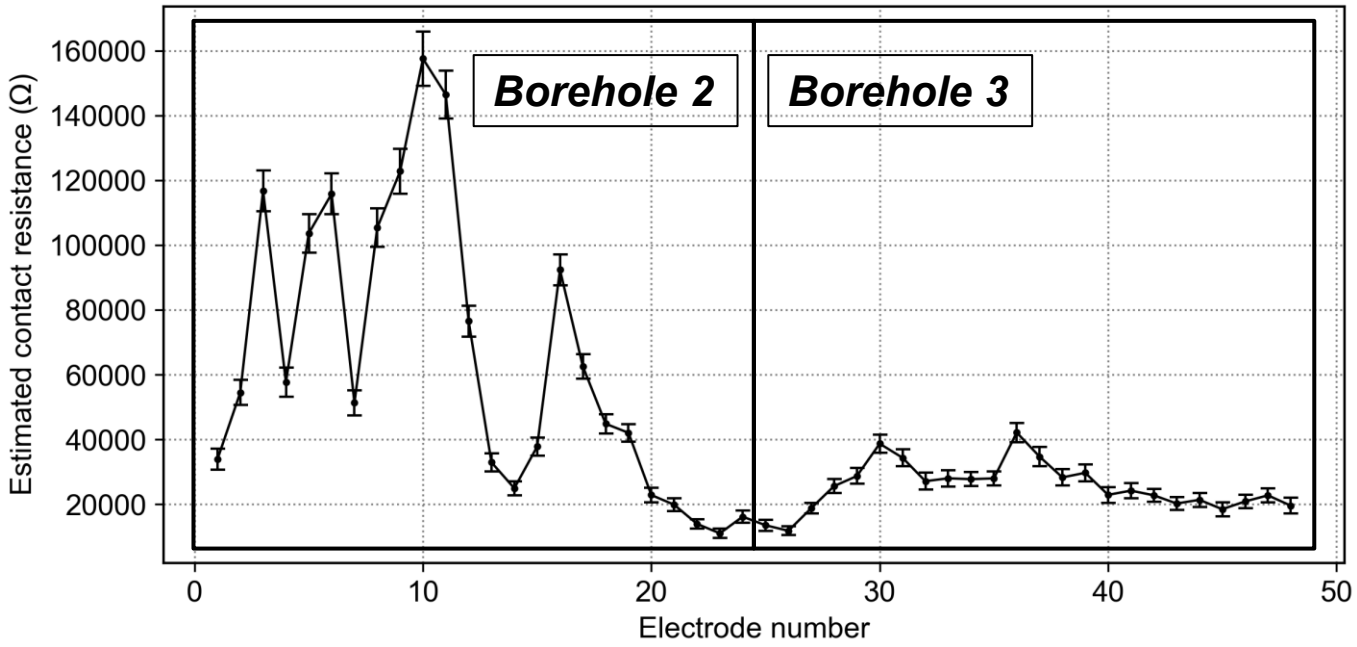

Estimation of contact resistances by least squares approach based on DAS-1 $V_{applied}/I_{applied}$ data assuming $R_s \ll R_{ci}$

Considers uncertainty of measured R_{AB} from **repeated current injections**

High contact resistances: might be underestimated or even above DAS-1 power capacity

Low contact resistances: values are highly reliable (validated with PSIP measurements)

Contact resistances

Comparison with contact resistances measured by PSIP

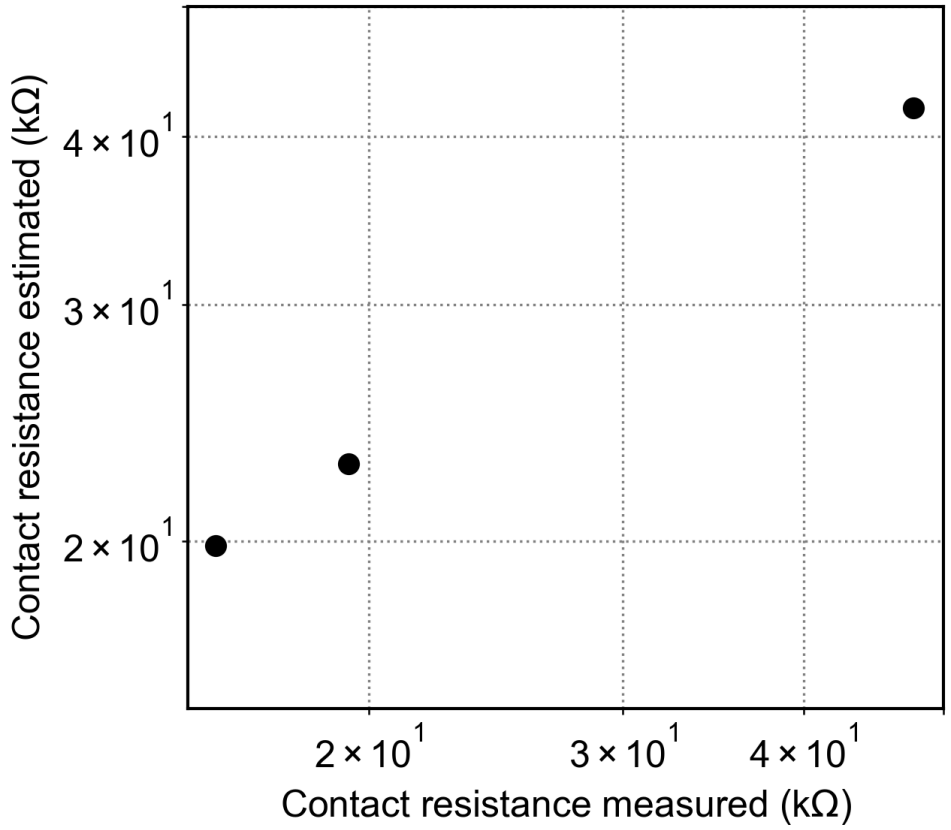

[Approach from Wang & Slater, 2019]

Estimation of contact resistances by least squares approach based on DAS-1 $V_{applied}/I_{applied}$ data assuming $R_s \ll R_{ci}$

Considers uncertainty of measured R_{AB} from **repeated current injections**

High contact resistances: might be underestimated or even above DAS-1 power capacity

Low contact resistances: values are highly reliable (validated with PSIP measurements)

PSIP profiling

MG Configuration

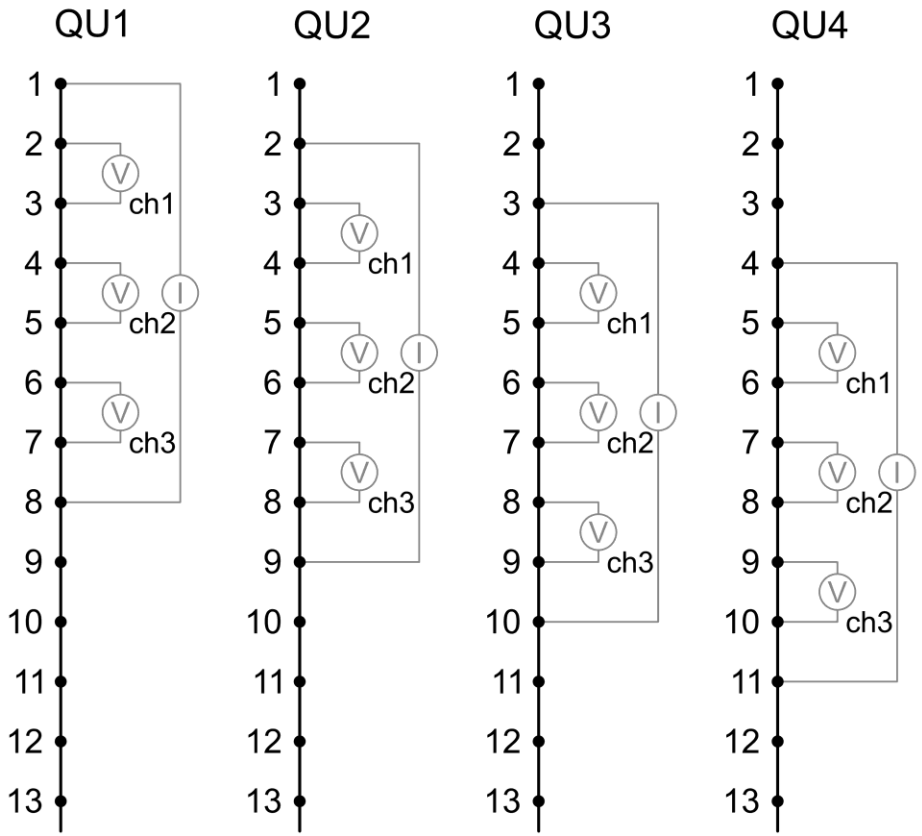

Frequency: 1.0 Hz

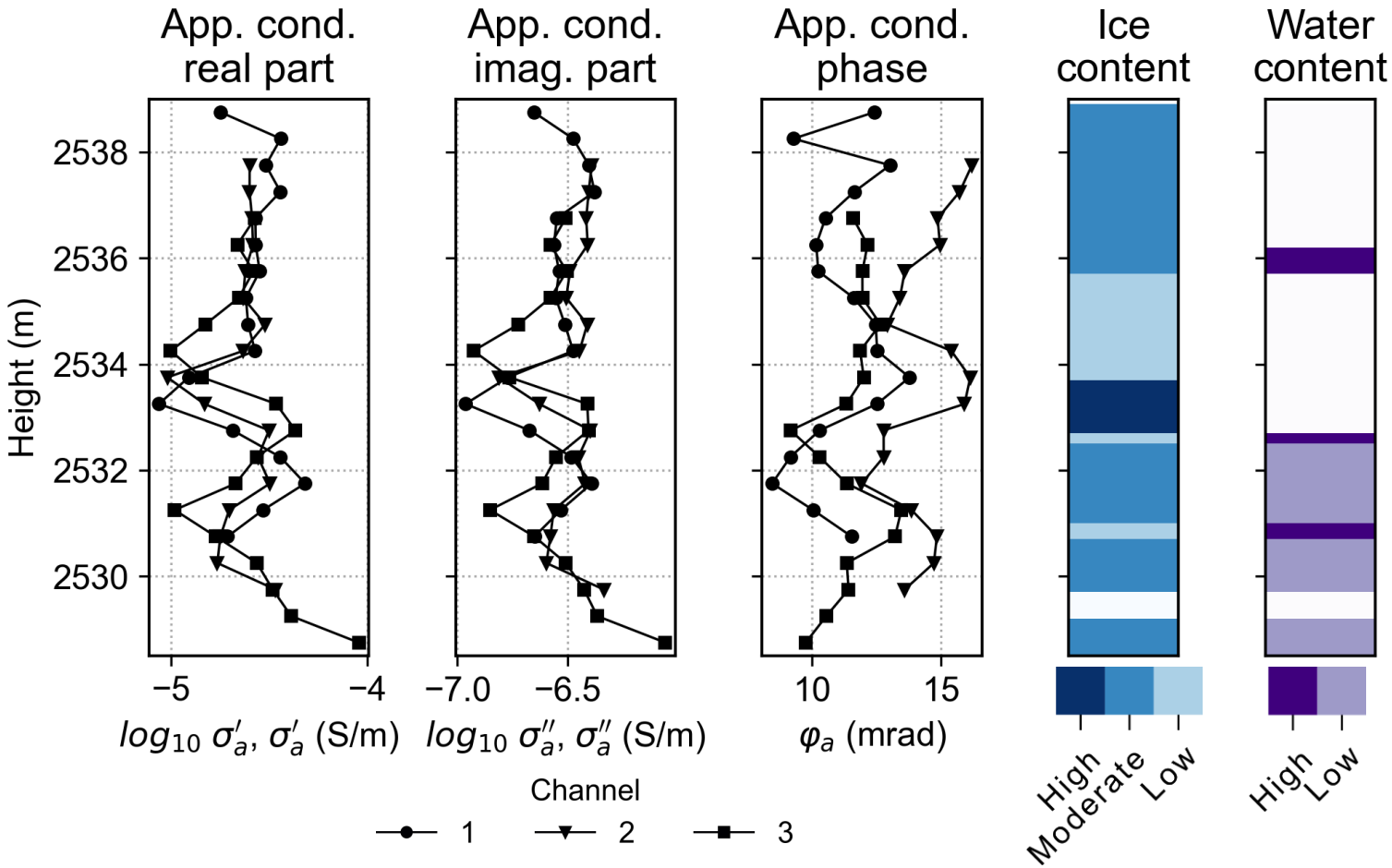

PSIP profiling

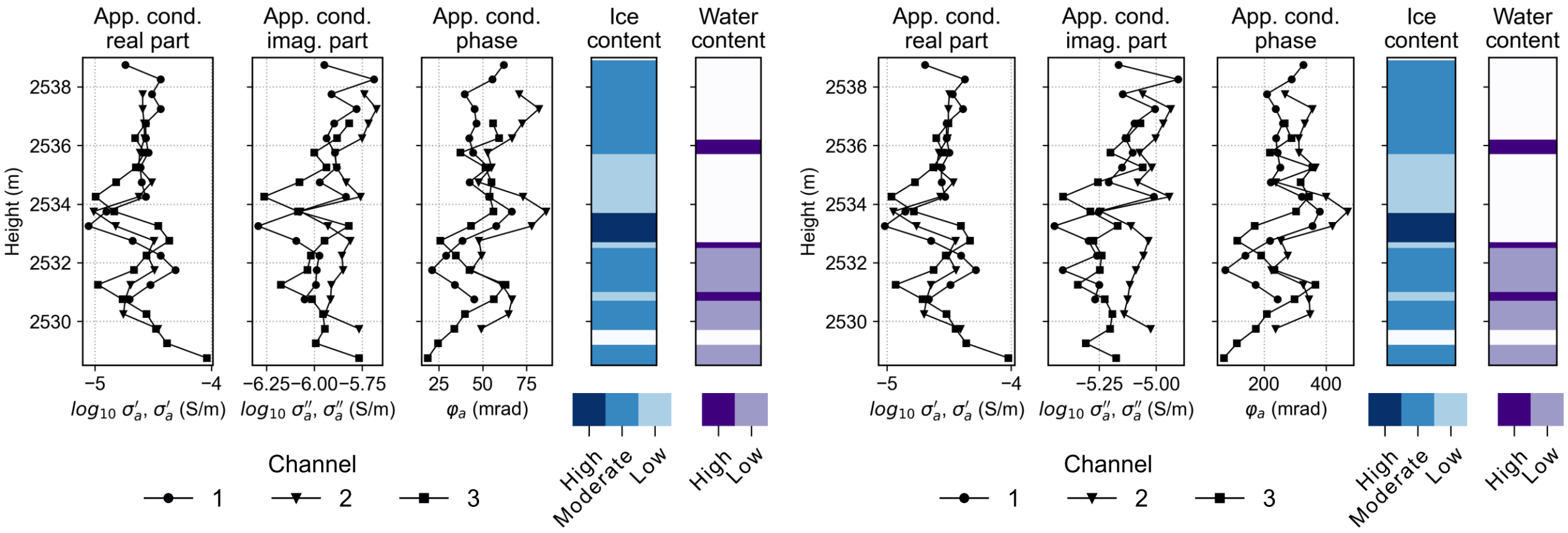

DAS-1 imaging data

Accumulation of positive impedance phase readings

Dipole-dipole sk-3

Dipole-dipole sk-0

1.0 Hz

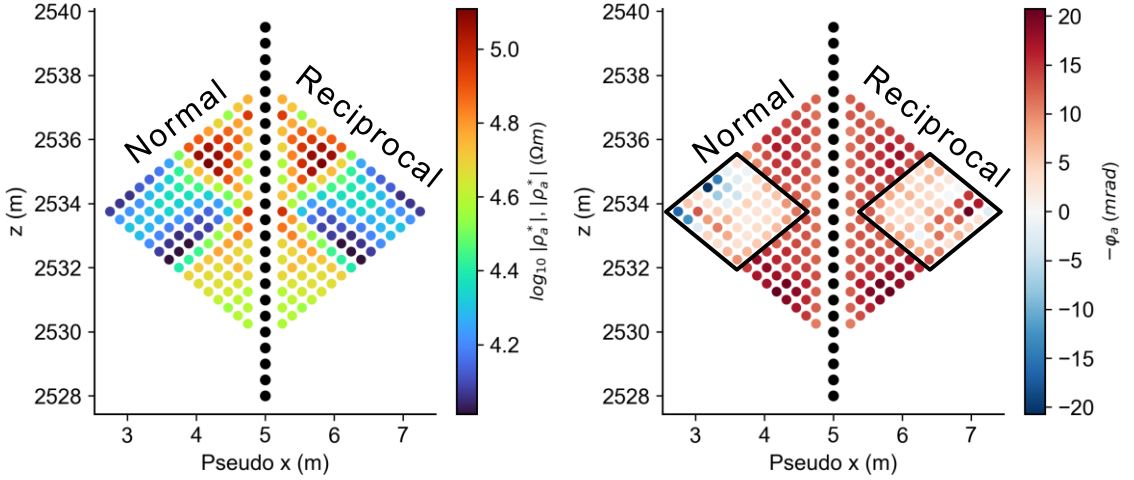

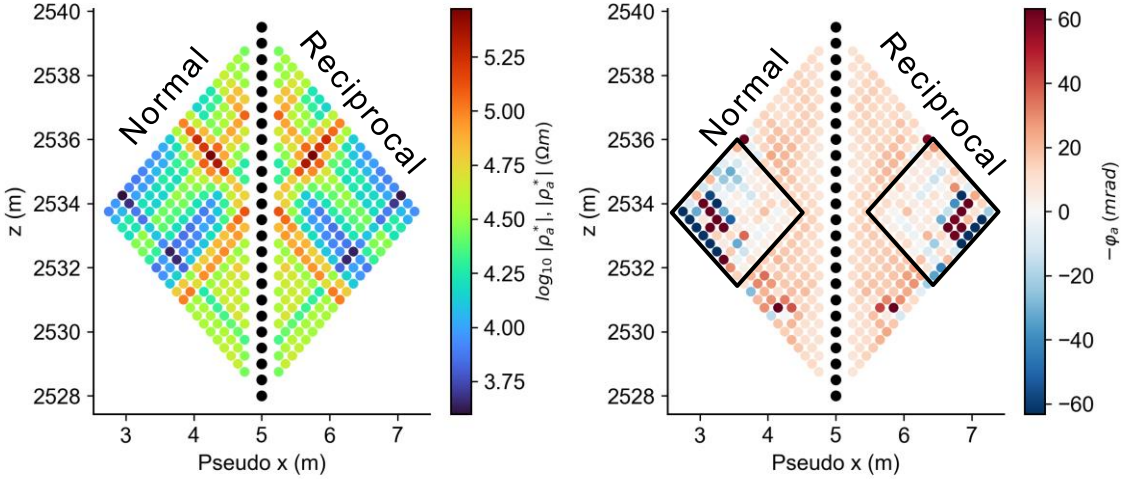

7.5 Hz

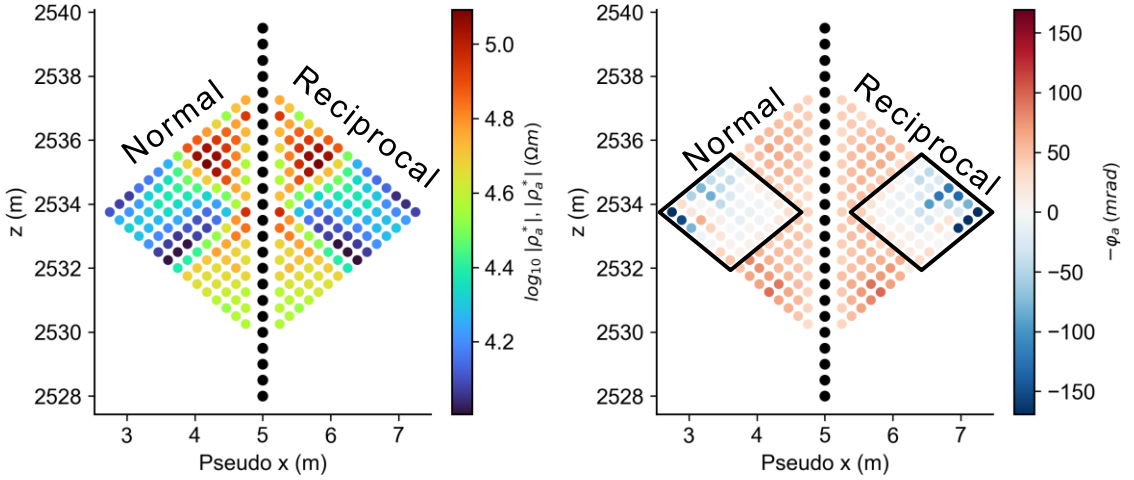

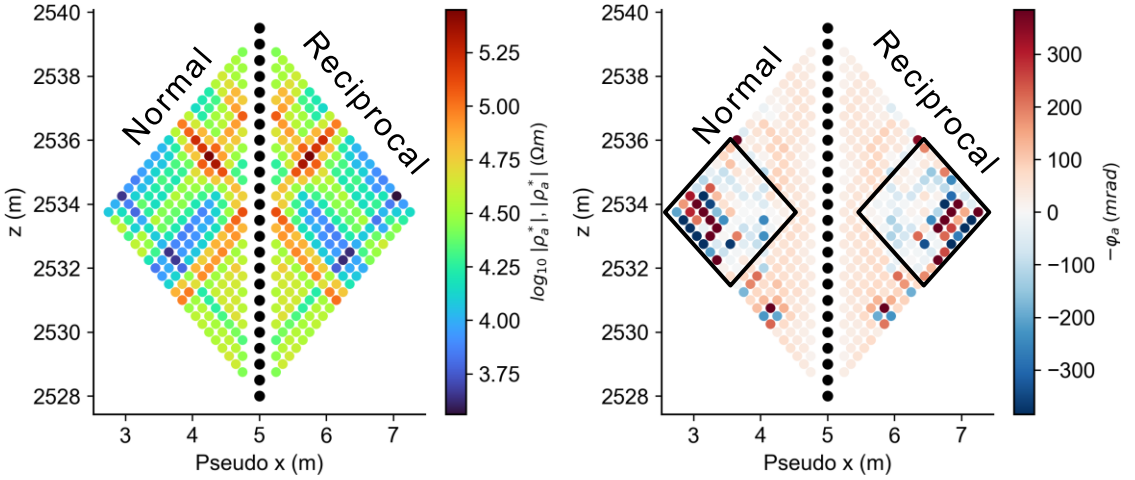

Numerical modeling dipole-dipole sk-0

Accumulation of positive impedance phase readings

Synthetic model

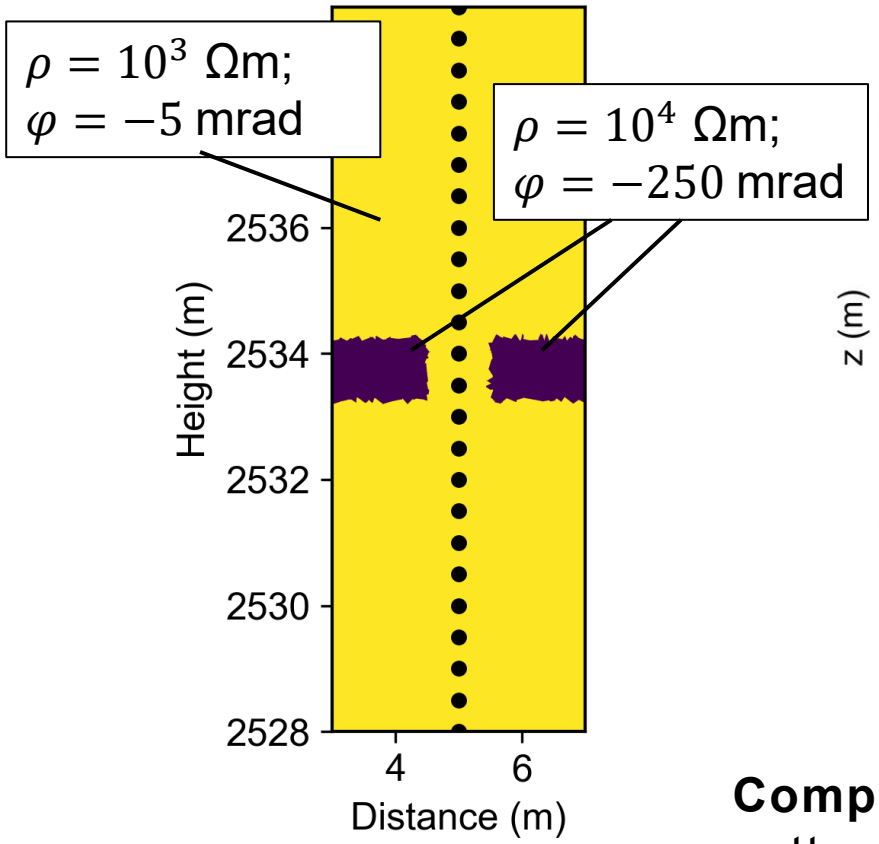

Pseudosections DD sk-0

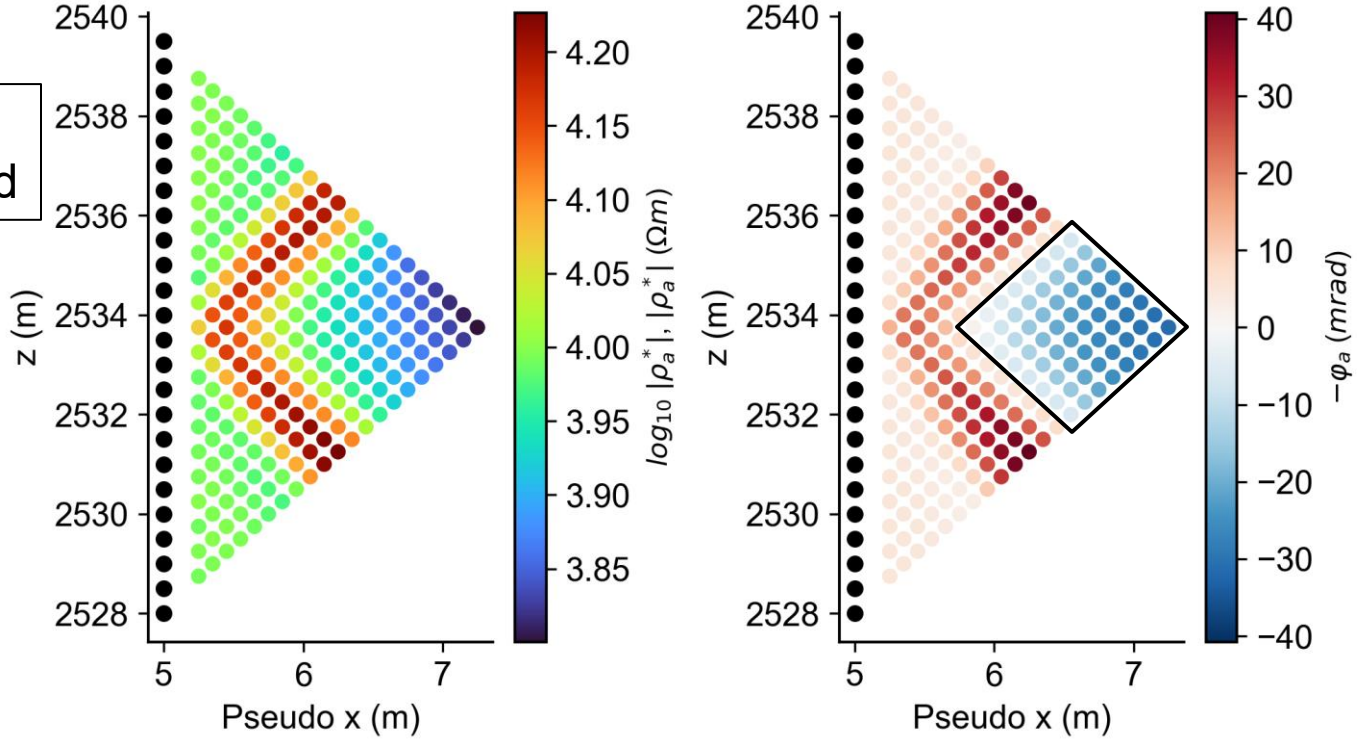

Comparison: Field data pseudosections show a very similar pattern as the pseudosections of the modelled data

Numerical modeling dipole-dipole sk-3

Accumulation of positive impedance phase readings

Synthetic model

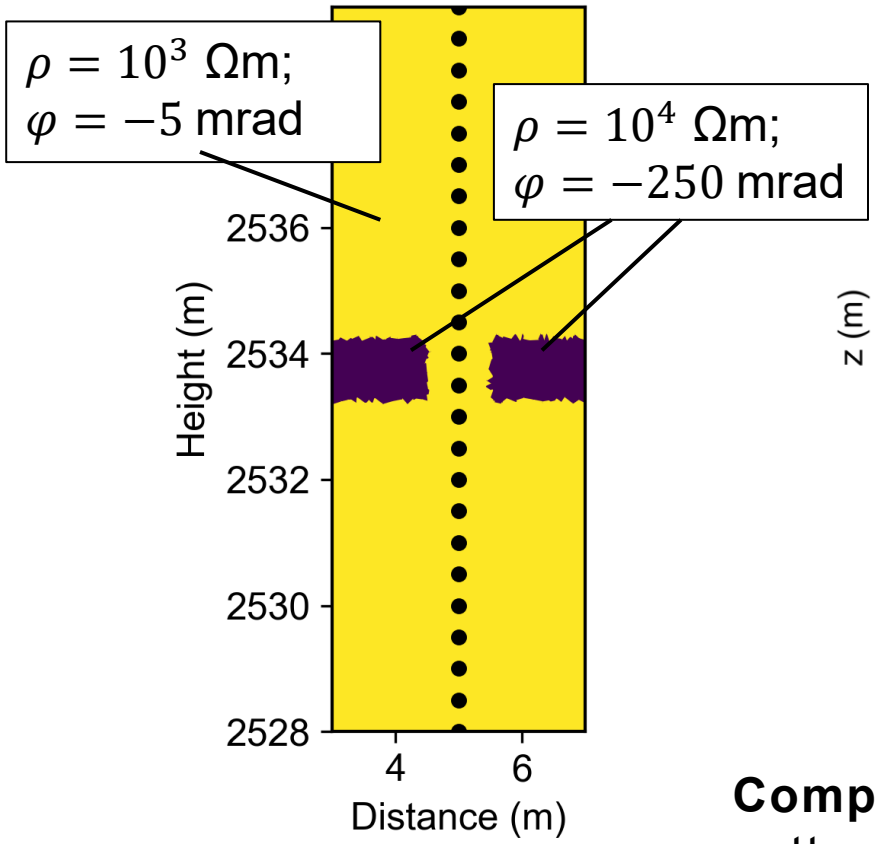

Pseudosections DD sk-3

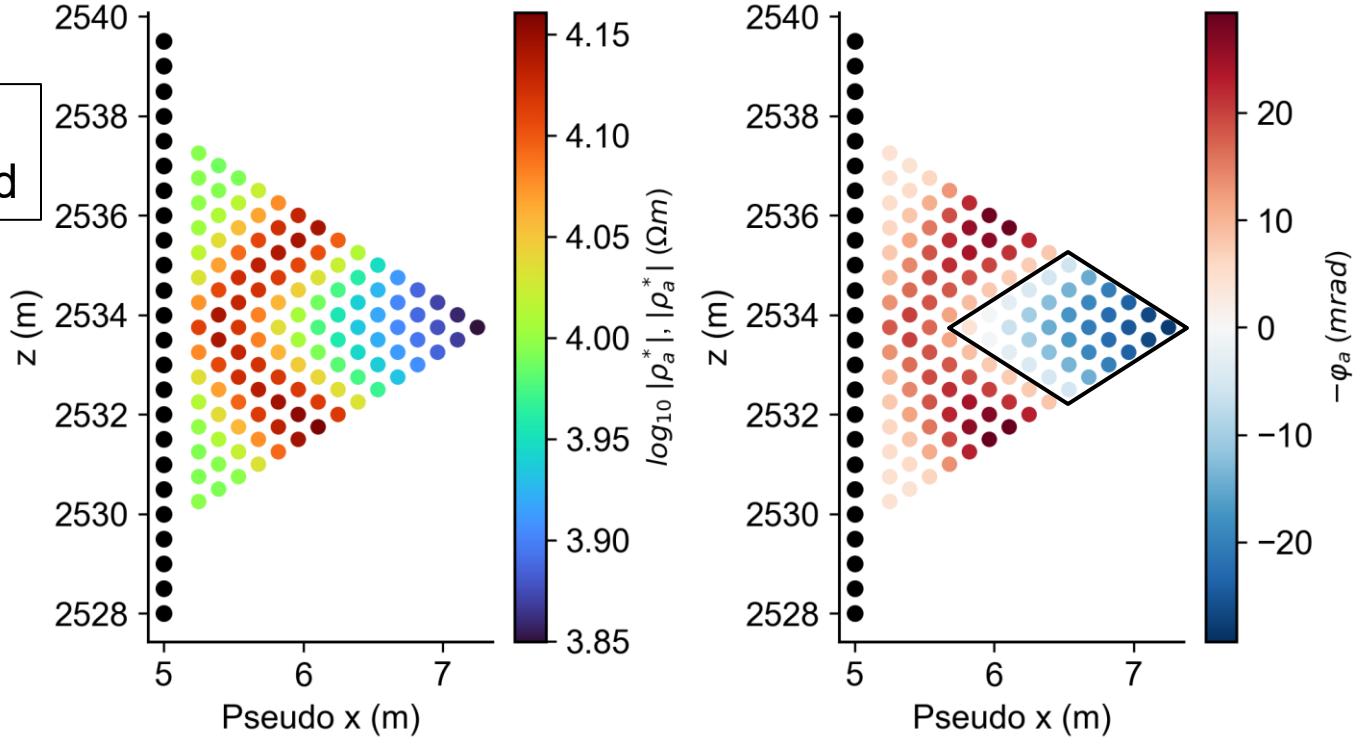

Comparison: Field data pseudosections show a very similar pattern as the pseudosections of the modelled data

Inversion results

Dipole-dipole sk-3

Dipole-dipole sk-0

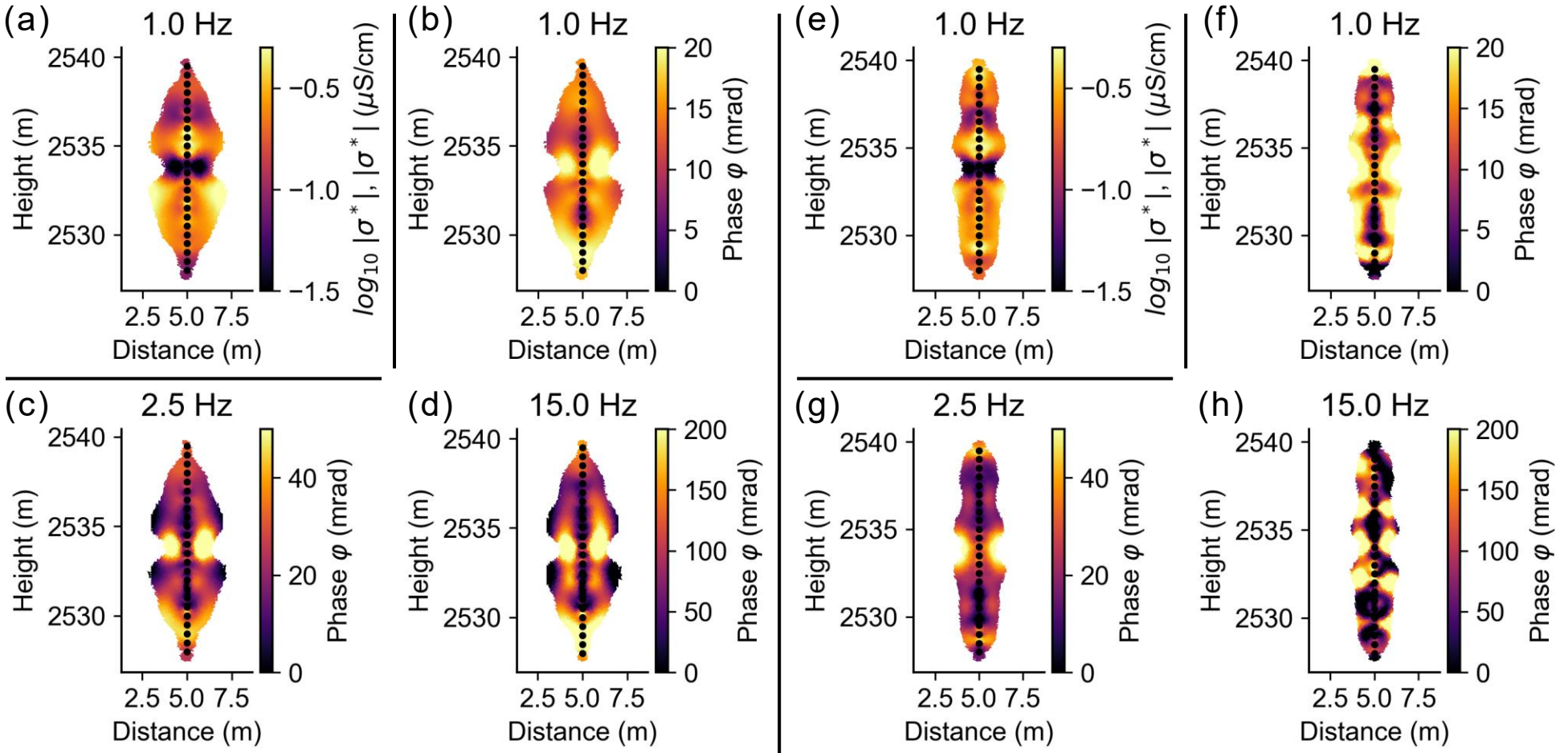

- Inversion after **keeping positive impedance phase** readings
- Results in **resistive and polarizable** (increased conductivity phase) **anomaly**
- Phase value **increase with increasing frequency**

Varying colorscale due to large difference in range of values

Conclusions experiment 3

1) **Large variations in conductivity magnitude and phase** along borehole in active rock glacier

2) Strong **negative IP effects** similar to tank experiment result from resistive and polarizable anomaly

3) **Resistive and polarizable anomaly** is correlated with maximum in ice content estimation

Overall conclusions

Experiments at different scales

(1) Borehole experiment

Meter scale

- **Lateral variations** in low-frequency **polarization** along borehole
- **Negative IP effects** due to resistive and polarizable anomaly

(2) Tank experiment

Decimeter scale

- **Similar negative IP effects** due to resistive and polarizable anomaly
- Allows to **validate polarization anomaly** with known geometry of the ice

(3) Rock samples experiment

Centimeter scale

- Effect in **thermal equilibrium** taking place in electric double layer
- Effect **during ice formation** due to charge separation

References

Binley, A., and Slater, L.: Resistivity and Induced Polarization: Theory and Applications to the Near-surface Earth, Cambridge University Press, Cambridge, https://doi.org/10.1017/9781108685955.003, 2020.

Blanchy, G., Saneiyan, S., Boyd, J., McLachlan, P., and Binley, A.: ResIPy, an intuitive open source software for complex geoelectrical inversion/modeling, Comput. Geosci., 137, 104423, https://doi.org/10.1016/j.cageo.2020.104423, 2020.

Grimm, R. E., and Stillman, D. E.: Field test of detection and characterisation of subsurface ice using broadband spectral-induced polarisation. Permafrost and Periglacial Processes, 26(1), 28–38, https://doi.org/10.1002/ppp.1833, 2015.

Kemna, A.: Tomographic inversion of complex resistivity –Theory and application. PhD thesis, Ruhr-University of Bochum, 2000.

Limbrock, J. K., Weigand, M., and Kemna, A.: Temperature Dependence of the Low-Frequency Electrical Properties of Partially Frozen Rocks, Journal of Geophysical Research: Solid Earth, 130, https://doi.org/10.1029/2024JB030870, 2025.

Maierhofer, T., Flores Orozco, A., Hilbich, and Hauck, C.: Spectral induced polarization measurements at different mountain permafrost landforms with varying ice contents, Geophysical Journal International, 244, 1–23, https://doi.org/10.1093/gji/ggag005, 2026.

Moser, C., Morra di Cella, U., Hauck, C., and Flores Orozco, A.: Spectral induced polarization survey for the estimation of hydrogeological parameters in an active rock glacier, The Cryosphere, 19, 143–171, https://doi.org/10.5194/tc-19-143-2025, 2025.

Moser, C., & Flores Orozco, A.: Low-frequency polarization of blank ice features in solid rocks, Geophysical Research Letters, 53, https://doi.org/10.1029/2025GL119116, 2026.

Mudler, J., Hördt, A., Kreith, D., Sugand, M., Bazhin, K., Lebedeva, L., and Radić, T.: Broadband spectral induced polarization for the detection of Permafrost and an approach to ice content estimation – a case study from Yakutia, Russia, The Cryosphere, 16, 4727–4744, https://doi.org/10.5194/tc-16-4727-2022, 2022.

Noetzli, J., Isaksen, K., Barnett, J., Christiansen, H. H., Delaloye, R., Etzelmüller, B., et al.: Enhanced warming of European mountain permafrost in the early 21st century, nature communications, 15, 10508, https://doi.org/10.1038/s41467-024-54831-9, 2024.

Petrenko, V. F.: Electrical properties of ice (No. CRREL-SR-93-20), Cold Regions Research And Engineering Lab Hanover Nh, 1993.

Sugand, M., Hördt, A., and Binley, A.: Estimating Permafrost Ice Content from Independent Frequency Inversion of High-Frequency IP Data: A Case Study from Heliport Mire, Abisko, Sweden, Geophysical Journal International, Accepted Manuscript, 1–22, 2026.

Wang, C., and Slater, L. D.: Extending accurate spectral induced polarization measurements into the kHz range: Modelling and removal of errors from interactions between the parasitic capacitive coupling and the sample holder, Geophysical Journal International, 218(2), 895–912, https://doi.org/10.1093/gji/ggz199, 2019.